Evidence Report:

Risk of Acute Radiation Syndromes due to Solar Particle Events

Human Research Program
Space Radiation Program Element

Approved for Public Release: date to be added by SMO

National Aeronautics and Space Administration
Lyndon B. Johnson Space Center
Houston, Texas

CURRENT CONTRIBUTING AUTHORS:

Lisa Carnell, PhD	**NASA Langley Research Center, Hampton, VA**
Steve Blattnig, PhD	**NASA Langley Research Center, Hampton, VA**
Shaowen Hu, PhD	**Wyle, Houston, TX**
Janice Huff, PhD	**Universities Space Research Association, Houston, TX**
Myung-Hee Kim, PhD	**Wyle, Houston, TX**
Ryan Norman, PhD	**NASA Langley Research Center, Hampton, VA**
Zarana Patel, PhD	**Wyle, Houston, TX**
Lisa Simonsen, PhD	**NASA Langley Research Center, Hampton, VA**
Honglu Wu, PhD	**NASA Johnson Space Center, Houston, TX**

PREVIOUS CONTRIBUTING AUTHORS:

Honglu Wu	**NASA Johnson Space Center**
Janice L. Huff	**Universities Space Research Association**
Rachel Casey	**Universities Space Research Association**
Myung-Hee Kim	**Universities Space Research Association**
Francis A. Cucinotta	**NASA Johnson Space Center**

Reference for original report: *Human Health and Performance Risks of Space Exploration Missions, (Jancy C. McPhee and John B. Charles, editors), NASA SP-2009-3405, 2009.*

Table of Contents

I. PRD RISK TITLE: RISK OF ACUTE RADIATION SYNDROMES DUE TO SOLAR PARTICLE EVENTS 4

II. EXECUTIVE SUMMARY 4

III. INTRODUCTION 5

A. Description of Acute Risks of Concern to NASA 5

B. Current NASA Permissible Exposure Limits 7

IV. EVIDENCE 10

A. Human Evidence 10

1. Reviews of Human Data in Patients and Accident Victims 10

2. Organ-Specific Manifestations of the Acute Radiation Syndrome 11

3. Hereditary and Fertility Effects 17

B. Ground-based Studies on Acute Radiation Effects 18

1. RBE and Dose Rate Studies in Mice, Rats, Ferrets, and Larger Species 18

2. RBE and Dose Rate Studies of Cell Inactivation 20

V. COMPUTER-BASED MODELING AND SIMULATION 20

A. Radiation-Induced Performance Decrement (RIPD) Models 21

B. Hematopoietic Response Models 23

C. Epidermal Response Models 26

VI. RISK IN CONTEXT OF EXPLORATION MISSION OPERATIONAL SCENARIOS 27

A. Cumulative Probability of a Solar Particle Event Occurrence during a Given Mission Period 27

B. Spectral Representation of Solar Particle Events 29

C. Temporal Profiles of Solar Particle Events 30

D. Shielding Material and Shielding Distribution of Spacecraft 31

E. Solar Alert and Monitoring 32

F. Acute Radiation Risk and BRYNTRN (Baryon Transport) Organ Dose Projection (ARRBOD) 32

G. Potential for Biological Countermeasures 33

VII. GAPS 48

VIII. CONCLUSION 48

IX. REFERENCES 49

X. TEAM **65**
IX. LIST OF ACRONYMS **66**

I. PRD Risk Title: Risk of Acute Radiation Syndromes due to Solar Particle Events

Crew health and performance may be impacted by a major solar particle event (SPE), multiple SPEs, or the cumulative effect of galactic cosmic rays (GCR) and SPEs. Beyond low-Earth orbit, the protection of the Earth's magnetosphere is no longer available, such that increased shielding and protective mechanisms are necessary in order to prevent acute radiation sickness and impacts to mission success or crew survival. While operational monitoring and shielding are expected to minimize radiation exposures, there are EVA scenarios outside of low-Earth orbit where the risk of prodromal effects, including nausea, vomiting, anorexia, and fatigue, as well as skin injury and depletion of the blood-forming organs (BFO), may occur. There is a reasonable concern that a compromised immune system due to high skin doses from a SPE or due to synergistic space flight factors (e.g., microgravity) may lead to increased risk to the BFO. The primary data available at present are derived from analyses of medical patients and persons accidentally exposed to acute, high doses of low-linear energy transfer (LET) (or terrestrial) radiation. Data more specific to the space flight environment must be compiled to quantify the magnitude of increase of this risk and to develop appropriate protection strategies. In particular, information addressing the distinct differences between solar proton exposures and terrestrial exposure scenarios, including radiation quality, dose-rate effects, and non-uniform dose distributions, is required for accurate risk estimation.

II. Executive Summary

The foundation of acute radiation syndrome (ARS) evidence is ground-based observations of humans who were exposed to high levels of ionizing radiation, in particular to gamma- or x-rays, in a short period of time. Data on ARS have been summarized in the literature and in numerous committee reports, including reports from the National Council on Radiation Protection (NCRP) and the National Research Council (NRC), which provide the foundation of evidence used by NASA for research plans and operational radiation protection strategies.

The risk of ARS from exposure to large solar particle events (SPEs) during space missions was identified during the early days of the human space program (NAS/NRC 1967). ARS symptoms can include hematopoietic, gastrointestinal, cutaneous, and neurovascular decrements. However, the ARS symptoms that appear in the prodromal phase post-exposure (e.g., nausea, vomiting, anorexia, and fatigue) are the most likely to be experienced based on estimated organ doses during extra-vehicular activity (EVA; free space or lunar operations) and could significantly impact mission success if adequate shielding is not reached in a timely manner (ICRP 2012).

Small- to medium-sized SPEs are known to occur quite often over the approximately 11-year solar cycle, but they are highly episodic and difficult to predict. Large mission-threatening events are rare. SPEs include low- to medium-energy protons, with the energy region of most importance to human spaceflight extending out to a few hundred MeV, as well as much smaller components of helium and heavy nuclei. During such events, the flux of protons with energy greater than 10 MeV may increase over background by 4 to 5 orders of magnitude for a period of several hours to a few days. The shapes of the energy spectra, as well as the total fluence, vary considerably from event to event. ARS has been well-defined for gamma- and X-ray exposures, both characterized as low-LET radiation. However, less is known about the acute effects from whole-body exposures to SPE protons, which are characterized by dynamic changes in energy

distribution, leading to dose rates that can vary several-fold between tissue sites throughout the human body. Additional radiobiology research is needed to understand how reduced immunity from large skin doses or other synergistic effects of spaceflight, such as microgravity, may alter dose thresholds for response as well as to identify and validate the effectiveness of medical countermeasures for proton irradiations.

Improvements in SPE forecasting and alert systems are needed to minimize operational constraints, especially for EVA. While radiation shielding is an effective mitigation to ARS, the high cost of shielding requires accurate estimates of the risk to ensure that sufficient protection is provided without overestimating shielding requirements.

NASA has developed several models for the probabilistic risk assessment of acute radiation syndrome from SPEs. These models include the improved spectral fit of SPEs over all energies and the analysis of any SPEs at a certain proton fluence based on the distribution of total fluence of the recorded SPEs. These models were built to fulfill National Research Council (NRC) recommendations from 2008 for the development of probabilistic approaches to modeling SPEs, *Managing Space Radiation Risk in the New Era of Space Exploration* (NRC 2008). In addition, nonlinear kinetics models of bone marrow stem cells and various blood system components have been developed to describe and provide accurate descriptions of human and other species responses to acute and chronic irradiation. These organ dose projection models are incorporated in a software package called ARRBOD for use by mission planners, radiation shield designers, and space operations to evaluate clinically significant deterministic health effects, including performance degradation in flight, from exposure to large SPEs.

III. Introduction

A. Description of Acute Risks of Concern to NASA

In contrast to the constant presence of GCRs in space, SPE exposures are sporadic and occur with little warning. During a SPE, the Sun releases a large amount of energetic particles. Although the composition of the particle type varies slightly from event to event, those of most concern for human missions on average consist of 96% protons, 4% helium ions, and a small fraction of heavier ions (NCRP 1989a; Cucinotta et al. 1994; Townsend et al. 1994; Kim et al. 1999). The intensity and the energy spectrum of an SPE vary throughout the course of the event, which lasts from a few hours to several days. Each event has distinct temporal and energy characteristics. The intensity of the event can be described by particle fluence, $F_{>E}$, which is the number of ions per unit area with energy greater than E, expressed as mega electron volts per nucleon (MeV/n). The energies of the protons are important because the range of penetration of these protons increases with energy. Protons with energies above 30 MeV have sufficient range to penetrate an EVA spacesuit and are used as a simple scaling parameter to compare different SPEs. The majority of SPEs observed in the last 50 years are relatively harmless to human health, with doses below 10 mGy requiring minimal shielding protection. However, SPEs that have the highest fluence of particles with energies above 30 MeV are of greatest concern for future missions outside the protection of the earth's magnetic field (Kim et al. 2011).

Figure 1 shows data that were collected in the modern era for the $F_{>30\ MeV}$ proton fluence (bottom panel) from large SPEs and the solar modulation parameter (Φ) (upper panel). The solar modulation parameter describes the strength of the sun's magnetic field with solar maximum at

Φ>1,000 MV (Kim et al. 2011). The various SPEs shown in Figure 1, which are characterized as large SPEs ($F_{>30\ MeV} > 10^8$ particles/cm^2), would contribute doses of 10 to 500 mGy for average shielding conditions. Although the dose resulting from the majority of SPEs is small, SPEs nonetheless pose significant operational challenges because the eventual size of an event cannot be predicted until several hours after the particles are initially detected. Extraordinarily large SPEs were recorded in November 1960, August 1972, and October 1989. In general, SPEs occur more often near solar maximum, but as Figure 1 shows, the correlation between event frequency and solar conditions is not precise (Shea and Smart 1990; Kim et al. 2011). To date, accurate short- or long-term prediction of SPEs has not been possible.

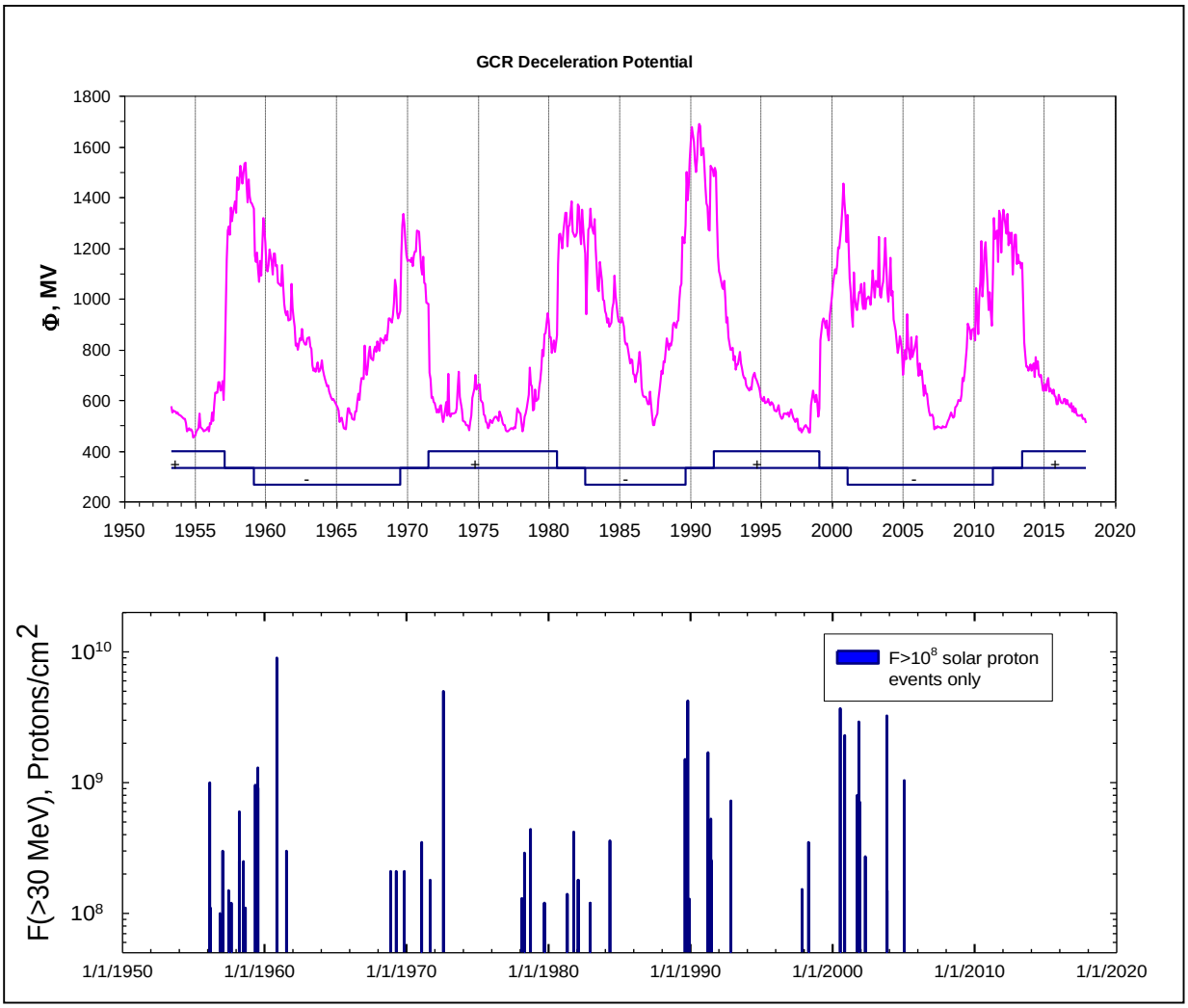

Figure 1. Historical data on fluence of protons above 30 MeV per cm^2 ($F_{>30\ MeV}$ from large SPEs relative to solar modulation parameter [Φ]). Only events with $F_{>30\ MeV} > 10^8$ protons/cm^2 are shown.

Without sufficient shielding protection for these large events, a whole-body dose of over 0.5 Gy (500 mGy) may be received over a period of several hours (Parsons and Townsend 2000; Kim et al. 2011), which would put humans at risk for development of ARS and could impact operations by affecting crew performance, leading to the possibility of mission failure. However, shielding

and operational, active dosimetry are effective countermeasures to SPEs inside spacecraft, making ARS extremely unlikely except in extended EVA or combined EVA and intra-vehicular activity (IVA) scenarios (Wilson 1997).

B. Current NASA Permissible Exposure Limits

Current permissible exposure limits (PELs) for short-term and career astronaut exposures to space radiation have been approved by the NASA Chief Health and Medical Officer as documented in NASA Standard 3001, Vol. 1, Revision A, 2014. The PELs provide the basis for setting requirements and standards for mission design and crew selection. Past reviews of evidence by the National Academy of Sciences (NAS) and the NCRP form the basis for the NASA PELs, including short-term limits that are imposed to prevent clinically significant deterministic health effects, including performance degradation in flight (NASA 2007, 2011, 2014). NAS first reviewed space flight issues in 1967 (NAS/NRC 1967) and conducted a further review in 1970 (NAS/NRC 1970) that led to the dose limits that were used at NASA until 1989. Extensive reviews of humans and experimental radiobiology data for ARS were provided to NASA by reports of the NCRP in 1989, 2000, and 2006 (NCRP 1989b, 2000, 2006). The report of the NAS in 1970 is the basis for the limits to the BFO that are currently used at NASA, which are instituted to protect the hematopoietic system from depletion below a critical limit. Dose limits for the prodromal risks were not advocated by the NAS or the NCRP for NASA missions in the past. However, the BFO limit likely occurs at doses below that of the threshold for prodromal effects, so adherence to the BFO 30-day limit protects against occurrence of ARS.

The current NASA dose limits for deterministic effects to the lens, skin, BFO, and circulatory system, which are given in units of Gray-equivalent (Gy-Eq), are listed in Table 1. The unit of Gray-equivalent is calculated using the relative biological effectiveness (RBE) values shown in Table 2 as described in NCRP Report No. 132 (2000) and is distinct from the unit of Sievert (Sv) that is used to project cancer risk. Note that while the Gray Equivalent quantity is used to limit these non-cancer effects (Table 1), the RBEs for central nervous system (CNS) non-cancer effects are largely unknown; therefore, a physical dose limit (mGy) is used, with an additional PEL requirement for particles with charge Z>10 (Table 1).

Doses to the BFO from an SPE event above 1 Gy are highly unlikely if crew members are able to reach a moderately shielded (5 to 10 g/cm2) location in a timely manner. Table 3, updated from Hu et al. (2009) using ARRBOD 2.0 with an exponential fitting scheme, presents estimates of several dosimetric quantities from three historically large SPEs (August 1972 SPE, October 1989 SPE, September 1989 SPE) for the total event spectra in interplanetary space calculated for a spacesuit during an EVA (an aluminum sphere of 0.3 gm/cm2 thickness), inside a typical equipment room of a spacecraft (an aluminum sphere of 5 gm/cm2 thickness) and with increasing quantities of shielding. These are total dose estimates over an entire event spectra, which exceeded 60 hrs for the August 1972 event.

Table 1. Dose Limits for Short-Term or Career Non-Cancer Effects (in mGy-Eq or mGy)
Note: RBEs for specific risks are distinct as described below.

Organ	30-day limit	1-year limit	Career
Lens*	1,000 mGy-Eq	2,000 mGy-Eq	4,000 mGy-Eq
Skin	1,500 mGy-Eq	3,000 mGy-Eq	6,000 mGy-Eq
BFO	250 mGy-Eq	500 mGy-Eq	Not applicable
Heart**	250 mGy-Eq	500 mGy-Eq	1,000 mGy-Eq
CNS***	500 mGy	1,000 mGy	1,500 mGy
CNS*** ($Z \geq 10$)	–	100 mGy	250 mGy

*Lens limits are intended to prevent early (<5 yr) severe cataracts, e.g., from a solar particle event. An additional cataract risk exists at lower doses from cosmic rays for sub-clinical cataracts, which may progress to severe types after long latency (>5 yr) and are not preventable by existing mitigation measures; however, they are deemed an acceptable risk to the program.
**Circulatory system doses calculated as average over heart muscle and adjacent arteries.
***CNS limits should be calculated at the hippocampus.
Reference: NCRP (2000) Recommendations of Dose Limits for Low Earth Orbit. NCRP Report 132, Bethesda MD.

Table 2. RBE for Non-Cancer Effects[a] of the Lens, Skin, BFO, and Circulatory Systems

Radiation Type	Recommended RBE[b]	Range
1 to 5 MeV neutrons	6.0	(4-8)
5 to 50 MeV neutrons	3.5	(2-5)
Heavy ions	2.5[c]	(1-4)
Proton > 2 MeV	1.5	-

[a] RBE values for late deterministic effects are higher than for early effects in some tissues and are influenced by the doses used to determine the RBE.
[b] There are not sufficient data on which to base RBE values for early or late effects by neutrons of energies <1 MeV or greater than about 25 MeV.
[c] There are few data on the tissue effects of ions with a Z>18, but the RBE values for iron ions (Z=26) are comparable to those of argon (Z=18). One possible exception is cataract of the lens of the eye because high RBE values for cataracts in mice have been reported.
Reference: NCRP (2000) Recommendations of Dose Limits for Low Earth Orbit. NCRP Report 132, Bethesda MD.

Table 3. Dosimetry quantities in interplanetary space from total event spectra of three large SPEs. (Note: EVA exposures (0.3 gm/cm^2) listed in Table are highly unlikely and illustrate the effectiveness of operational protocols where crew would shelter for the majority of event duration which can last for several days.)

Dosimetry quantities	August 1972 SPE				October 1989 SPE				September 1989 SPE			
	EVA 0.3 g/cm^2	Spacecraft 5 g/cm^2	10 g/cm^2 shielding	25 g/cm^2 shielding	EVA 0.3 g/cm^2	Spacecraft 5 g/cm^2	10 g/cm^2 shielding	25 g/cm^2 shielding	EVA 0.3 g/cm^2	Spacecraft 5 g/cm^2	10 g/cm^2 shielding	25 g/cm^2 shielding
D_{skin}, cGy	2859.27	241.11	20.75	1.74	2416.88	134.75	22.99	5.21	716.83	49.86	9.92	2.56
$G_{stomach}$, cGy-Eq	41.72	17.00	3.54	0.70	43.43	24.98	9.89	3.42	18.61	11.25	4.82	1.81
G_{BFO}, cGy-Eq	138.65	46.34	7.52	1.11	95.70	45.49	15.04	4.63	37.94	19.32	7.05	2.39
E, cSv	343.47	67.19	9.64	1.89	222.47	52.54	15.53	5.05	75.81	21.48	7.18	2.56
Total time, hrs	63				81				40			

Tissue-specific dose estimates for females and males (in Gy) for the August 1972 King event are presented in Table 4. These numbers were generated using Oltaris (https://oltaris.nasa.gov/) with FAX and MAX anatomical models. The GI dose is computed as the average dose received by the small intestine, stomach, and colon. Note the rapid attenuation of tissue dose with increasing quantities of shielding. Design and operational requirements, including access to storm shelters with thicker shielding, will aim to minimize exposures to less than 250 mGy-Eq to the BFO, thus limiting health risks to the crew.

Table 4. Total tissue dose accumulation for the August 1972 SPE calculated using the Oltaris web-based analysis tool. (Note: EVA exposures (0.4 gm/cm^2) listed in Table are highly unlikely and illustrate the effectiveness of operational protocols where crew would shelter for the majority of event duration which can last for several days.)

Shielding Thickness	0.4 g/cm^2	5 g/cm^2	10 g/cm^2	20 g/cm^2	0.4 g/cm^2	5 g/cm^2	10 g/cm^2	20 g/cm^2
Organ Specific Dose (Gy)	**Female**				**Male**			
Skin	27.98	2.74	0.71	0.11	28.20	2.76	0.72	0.11
BFO	1.43	0.39	0.14	0.03	1.01	0.29	0.11	0.03
Brain	1.55	0.51	0.20	0.05	1.30	0.45	0.17	0.04
Hippocampus	1.04	0.38	0.15	0.04	0.92	0.34	0.14	0.04
Ovaries	0.28	0.12	0.06	0.02	3.95	0.92	0.30	0.06
GI	0.63	0.23	0.09	0.03	0.49	0.19	0.08	0.02
Small_Intestine	0.57	0.21	0.09	0.02	0.44	0.17	0.07	0.02
Stomach	0.53	0.20	0.09	0.02	0.49	0.19	0.08	0.02
Colon	0.81	0.28	0.11	0.03	0.54	0.20	0.08	0.02
Adrenals	0.26	0.11	0.05	0.02	0.14	0.07	0.04	0.01
Bladder	0.37	0.15	0.06	0.02	0.36	0.14	0.06	0.02
Bone	2.27	0.56	0.20	0.04	1.75	0.45	0.16	0.04
Breast	4.08	1.02	0.34	0.06	1.31	0.41	0.15	0.04
Esophagus	0.53	0.21	0.09	0.03	0.42	0.17	0.08	0.02
Heart	0.44	0.18	0.08	0.02	0.60	0.23	0.10	0.03
Kidneys	0.43	0.17	0.08	0.02	0.33	0.14	0.06	0.02
Lens	10.76	1.85	0.54	0.09	12.57	1.82	0.52	0.09
Liver	0.67	0.24	0.10	0.03	0.44	0.17	0.07	0.02
Lungs	1.74	0.55	0.20	0.05	0.94	0.33	0.13	0.03
Muscle	1.98	0.57	0.20	0.04	1.91	0.55	0.20	0.04
Pancreas	0.26	0.11	0.05	0.02	0.15	0.07	0.04	0.01
Retina	3.27	0.87	0.29	0.06	0.27	0.11	0.05	0.02
Salivary_Glands	5.99	1.13	0.35	0.06	2.74	0.76	0.26	0.05
Spleen	0.68	0.25	0.10	0.03	5.94	1.09	0.34	0.06
Thymus	1.51	0.48	0.18	0.04	0.52	0.20	0.08	0.02
Thyroid	2.39	0.64	0.22	0.05	0.51	0.20	0.09	0.03
Trachea	1.44	0.45	0.17	0.04	1.18	0.38	0.14	0.03
Uterus	0.23	0.10	0.05	0.02	1.05	0.35	0.14	0.03

IV. Evidence

A. Human Evidence

The human evidence presented in this section is Category III unless otherwise noted.

1. Reviews of Human Data in Patients and Accident Victims

ARS involves exposure to high doses of radiation received over a large portion of the body in a very short window of time. Scenarios where this type of exposure could occur include nuclear power plant accidents, mishaps with irradiations used for sterilization purposes, military personnel in the event of a nuclear bomb detonation, and the general population should a terrorist attack occur that involves nuclear devices (Waselenko et al. 2004; Pellmar et al. 2005). Evidence of ARS in humans from low-LET radiation, such as gamma- or X-ray exposures, has been thoroughly reviewed and documented in the reports that have been generated by regulatory bodies such as the NAS, the National Council on Radiation Protection (NCRP), the International Commission on Radiological Protection (ICRP), the National Research Council (NRC), and the U.S. Nuclear Regulatory Commission (NAS/NRC 1967; NCRP 1982, 1989a, 1993, 2000; Baum et al. 1984; Evans et al. 1985;ICRP 2000, 2002, 2012; NRC 2008) (Category IV). Data accumulated over the last half-century that were used in the construction of the dose threshold for ARS were derived from the following studies: studies on the Japanese atomic bomb survivors (Ishida and Matsubayashi 1948; Ohkita 1975;Oughterson and Warren 1956), case studies of nuclear accident victims (Blakely 1968; Vodopick and Andrews 1974;Gilberti 1980), and records of total-body irradiated therapy patients for cancer and other diseases (Adelstein and Dealy 1965;Brown 1953; Warren and Grahn 1973). More recent events include the Chernobyl accident in 1986 (Bouville et al. 2006), an accident that occurred in Tokai-mura, Japan, in 1999 (Hirama et al. 2003), and the death of a Russian citizen after a possible internal overdose of radioactive materials as reported in the media in 2006.

ARS appears in various forms and has different threshold doses for onset of the possible effects. A previous definition of the threshold dose consisted of an exposure below which clinically significant effects do not occur (NCRP 2000). However, the ICRP has recently redefined a threshold dose as the dose required to cause a 1% incidence of an observable effect (ICRP 2007, 2012).

Radiation exposure induces physiological responses in many organ systems such as the hematopoietic, immune, reproductive, circulatory, respiratory, musculoskeletal, endocrine, nervous, and digestive systems, as well as the urinary tract, skin, and eye. However, the early effects (from the first hours to several weeks after exposure) are mainly manifested in the hematopoietic, cutaneous, gastrointestinal, and neurovascular systems (ICRP 2012). The threshold whole-body dose for ARS is approximately 0.1 to 0.2 Gy for radiation that is delivered under acute conditions where dose rates exceed 1 Gy/hr (ICRP 2012). At lower dose rates, a reduction in effects (which are described below) is seen. People at the extremes of age (children < 12 years and adults > 60 years) may be more susceptible to irradiation and have a lower LD50/60 (Hall 2006)

Doses that are in the range of 0.5 to 1 Gy cause minor acute damage to the hematopoietic system and mild prodromal effects (nausea, vomiting, anorexia, and fatigue) in a small number of irradiated persons (Anno et al. 1989). In the acute dose range of 1 to 2 Gy, prodromal effects and

injury to the hematopoietic system increase significantly; however, most victims will probably survive, with only 5% lethality in a population after doses of about 2 Gy (NAS/NRC 1967; McFarland and Pearson 1963). Survival is also possible within the dose range of 2 to 3.5 Gy, but prodromal effects become more pronounced, decreasing in latency and increasing in severity. As the dose reaches about 3.25 Gy, 50% of exposed people may die within 60 days if appropriate medical care is not administered (Lushbaugh 1969). From 3.5 to 5.5 Gy, symptoms are even more severe and affect nearly all who are exposed. If untreated, 50% to 99% of those who are exposed may die primarily because of extensive injury to the hematopoietic system that is manifested by overwhelming infections and bleeding (NAS/NRC 1967; Lushbaugh 1969; Messerschmidt 1979). At this dose range, permanent sterility occurs in both males and females (Paulsen 1973; NCRP 1989a).

Responses to doses between 5.5 and 7.5 Gy begin to reflect the combined effects of gastro-intestinal and hematopoietic damage. Survival is almost impossible without a compatible bone marrow transplant and/or extensive medical care. Nearly everyone who is irradiated at these doses suffers severe prodromal effects during the first day after exposure. When doses range between 7.5 and 10 Gy, injuries are much more severe due to a greater depletion of bone marrow stem cells (Adelstein and Dealy 1965; Lushbaugh 1962), increased gastrointestinal damage, and systemic complications from bacterial endotoxins entering the blood system.

Doses that are between 10 and 20 Gy produce early post-exposure renal failure (Lushbaugh 1974). Death results in fewer than 2 weeks from septicemia due to severe gastrointestinal injury, which is complicated by complete bone marrow damage and the cessation of granulocyte production (Lushbaugh, 1962). Above approximately 13 Gy, death may occur sooner from electrolyte imbalance and dehydration due to vomiting and diarrhea, especially in hot and humid conditions. Extremely severe gastrointestinal and cardiovascular damage causes death within 2 to 5 days after doses of 20 to 23 Gy (Lushbaugh 1969).

2. Organ-Specific Manifestations of the Acute Radiation Syndrome

The manifestation of ARS reflects the disturbance of physiological processes of various cellular groups damaged by radiation. Hematopoietic cells, skin, intestine, and vascular endothelium are among the tissues of the human body most sensitive to ionizing radiation. Most ARS effects are directly related to these tissues, as well as the coupled regulation and adaptation systems (nervous, endocrine, cardiovascular systems) (Guskova et al. 2001). Four sub-syndromes are identified: hematopoietic syndrome, cutaneous syndrome, gastrointestinal syndrome, and neurovascular syndrome. It is generally agreed that there are three phases in the development of the ARS: the prodromal phase, the latent phase, and the manifest phase. The severity and duration of each of these phases are dependent on the dose and dose rate. The prodromal phase refers to the first 48 hours after exposure, but it may persist for up to 6 days (Alexander et al. 2007). The syndromes are dose-dependent and include hematopoietic depression, gastrointestinal distress (nausea, vomiting, and/or diarrhea), and neurological symptoms (including fatigability, weakness, headache, impaired cognition, disorientation, ataxia, seizures, and hypotension). The latent phase lasts about 2 to 20 days, with a seeming improvement of most syndromes (except cytopenia) and duration correlating inversely with the absorbed dose. The manifest phase lasts from 2 to 60 days, with signs and symptoms expressed by various organs and profound immune suppression predisposing the body to infection and sepsis. This phase is critical for radiation injury. Most

patients surviving this phase will recover but are still at risk for intermediate effects such as pneumonitis and late effects (NCRP 2006; Guskova et al. 2001).

Based on the historical record of SPE fluence and likely shielding conditions, the most probable ARS effects from SPE exposure during spaceflight that can potentially affect mission success are the clinical symptoms associated with the prodromal phase of mild hematopoietic syndrome (nausea, vomiting, anorexia, and fatigue) occurring within the first 48 hrs following exposure, along with skin injury and depression of the BFOs (NAS/NRC 2006; Wilson et al. 1997). In general, symptoms develop within a few hours of radiation exposure and rarely exceed 24 hrs following low-LET radiation exposure (Fajardo et al. 2001). Exposure to higher doses results in greater severity, early onset, and longer duration of the symptoms (Anno et al. 1996). During spaceflight, the potential for a higher dose to the skin with associated changes in immune status may occur due to the inhomogeneous dose distribution associated with SPE exposure that may alter the threshold dose and time course for ARS. From ground-based observations, it is known that recovery from ARS can be hindered by changes in immune status, including those resulting from combined skin burns and other trauma (Fliedner et al. 2001). Therefore, understanding the effects of a higher skin exposure relative to the BFO on the hematopoietic and immune systems is important, as is the potential impact of microgravity and other spaceflight-associated changes to the immune system.

Significantly smaller amounts of data are available for prodromal effects from continuous exposure at lower dose rates. The current knowledge that has been collected from studies on victims who were exposed to radioactive fallout following the testing of nuclear devices and to other sources (Kumatori et al. 1980; Cronkite et al. 1956) is that dose rates of perhaps less than a few tens of mGy/h are probably not sufficient to cause ARS. However, continuous dose rates of around 100 mGy/h are probably high enough to cause significant vomiting within a period of approximately 1 day. Accordingly, between a few tens of mGy/h to approximately 100 mGy/h, a considerable amount of uncertainty exists concerning the human response to continuous radiation exposure, which is likely due to variations in the sensitivity of individuals as well as the quality of the very limited amount of existing data.

a. Hematopoietic Syndrome

Hematopoietic syndrome is characterized by a drop in the number of blood cells, generally at doses above 1 Gy to the bone marrow; however, mild symptoms may occur with doses as low as 0.3 Gy in susceptible individuals. The effects of radiation on hematopoiesis have been well-characterized in humans and animals for several decades (Bond et al. 1965). This is due to the pioneering work of applying the radiation ablation technique to identify hematopoietic stem cells (HSCs) (Till and McCulloch 1961), a small pool of pluripotent cells residing in bone marrow of the skeleton. While they have unlimited replication and pluripotent differentiation potential, HSCs are very radiosensitive. Their D_0 (the dose required to reduce the surviving fraction to 37% of that associated with the previous dose) was determined experimentally (in vivo and in vitro) to be between 0.6 and 1.6 Gy (Fliedner et al. 2002). Studies on human victims of radiation accidents indicate that the hematopoiesis system cannot recover from a traumatic event that kills more than 99% of these cells and that the resulting damage can only be overcome by a timely transfusion of compatible HSCs. On the other hand, lower doses of radiation will leave a sufficient number of these self-renewing cells intact, such that complete recovery can be achieved with time (Fliedner et al. 2002).

The manifestation of the hematopoietic syndrome is different in specific cell lineages. This is due to variations in compartment transit times, the mean and ranges of the quantities of mature cells in the peripheral blood, and the mean cell lifetimes of different cell lineages.

Normal human erythrocytes are radioresistant and have a lifespan on the order of 120 days. Therefore, even after a complete ablation of all erythropoietic development, the decline of erythrocytes in peripheral blood is about 1:120 per day, and after 30 days, the blood erythrocyte concentration declines to about 70% of normal values. Therefore, even after moderate- or high-dose total body irradiation (TBI) or partial body irradiation (PBI), anemia is usually not a significant clinical problem (Fliedner et al. 2001). On the other hand, reticulocyte lifespan in blood is about 1-3 days, and cell counts after radiation exposure show modulations similar to those of granulocytes and other radiosensitive cells.

Granulocytes are also radioresistant, but they disappear from the blood in a random fashion with a half-life of 6.6 hours (Fliedner et al. 2001). A unique feature of granulopoiesis is that a reserve pool exists in the bone marrow, where mature granulocytes can stay for a period of time depending on the demand in the peripheral blood (Babior and Golde 2001). It is known that the total transit time from the stem cell to the mature granulocyte in the marrow is 9–10 days. As mature granulocytes are radioresistant, after exposure, the granulocyte concentration in blood does not decrease immediately but increases to a magnitude proportional to the absorbed dose in the early stage (i.e., granulocytosis). For lethal doses, the granulocytes are completely depleted from blood between days 5 and 6; for moderate dose, the granulocyte concentration declines until reaching an abortive rise at around day 10, followed by a nadir around days 25-30 and a subsequent recovery (Fliedner et al. 2002). The dynamics of granulocyte cell counts in blood after radiation exposure reveals the extent of hematopoietic damage (Hu and Cucinotta 2011b). It has been established that all types of granulocytes (neutrophils, eosinophils, and basophils) are important to provide immune protection to the body. In animal experiments, the time of severe granulopenia is closely related to the species-dependent time of lethality (Bond et al. 1965). It is therefore essential to provide supportive care to victims to fight infections during the granulopenia period and apply techniques such as cytokine and cellular therapies to promote granulocyte proliferation (Singh et al. 2012).

The dynamics of platelets (thrombocytes) in blood after radiation exposure is very similar to that of granulocytes. Lethal doses also induce “essentially irreversible” injury to the thrombopoietic system and cause declining platelet counts progressively and rapidly to critical low levels below 50,000 per mm^3 within 10-12 days, which corresponds to the maximum lifespan of a platelet. For moderate doses, the pattern of the dynamics of platelets is characterized by a slowly declining shoulder lasting 10 to 15 days after exposure, followed by a nadir between 25 and 30 days and final recovery beyond day 30 and 35 (Fliedner et al. 2002). Thus, the severity and duration of thrombopenia are dose-dependent, and a quantitative relationship between platelet counts and the absorbed dose of an exposed victim can be established based on previous accidental patient data (Smirnova 2012). Reduced platelet counts in patients are clinically manifested by an increased tendency for bleeding. Therefore, it is important to provide medical support and therapeutic interventions to help patients survive through the period of reduced platelet concentrations.

Although the average lifespan of a lymphocyte in blood is about 4.4 years (Fliedner et al. 2002), lymphocytes are the most radiosensitive cell in peripheral blood. A radiation exposure resulting in a severe or lethal hematopoietic syndrome is characterized by a marked initial lymphocyte depression within the first hours. It has been proposed that this high sensitivity is due in part to the migration of lymphocytes from the circulation to lymph tissues and vice versa

(Fliedner et al. 2001), or to the radiation-induced apoptosis of mature lymphocytes in peripheral blood (Belka et al. 1998). In contrast to other cell lineages, mature lymphocytes recirculate between the blood vessels and lymphatic vessels (Gowans 1959). The capillary bed where lymphocytes transit from blood to the lymphatic tissue and back to the blood is highly sensitive to radiation (Stodtmeister et al. 1956). Due to these characteristics of the lymphopoietic system, monitoring the changes in lymphocyte counts after exposure is regarded as the most practical and best laboratory test to estimate radiation dose (Dainiak 2002). There are two widely used empirical methods for early estimation of the exposed dose after radiation accidents (Blakely et al. 2005). Past accidental records indicate that full recovery of normal lymphocyte levels in blood takes longer than other cell lineages (Hu et al. 2012). All types of lymphocytes are important components of the immune system, and lymphopenia reduces the body's capability to handle exogenous and endogenous cytotoxic agents.

b. Cutaneous Syndrome

Cutaneous syndrome describes the complex pathophysiological response of the skin following radiation exposure. Skin damage is commonly associated with ARS, but it is also possible to receive skin damage without development of ARS from exposure to beta radiation or x-rays. The skin epidermis is the outermost surface of the body and functions as a barrier to protect from dehydration, mechanical stress, and infections. It undergoes constant turnover through continuous self-renewal and differentiation of a small population of epidermal stem cells (Blanpain and Fuchs 2009). These underlying proliferative cells are sensitive to radiation and can be injured and depleted by high-dose exposures. Radiation damage to skin includes erythema, pigmentation, and dry and moist desquamation in the early phase (< 4 weeks) and atrophy and fibrosis (or necrosis) in the later phase (> 6 weeks) (NCRP 1989b). The ED_{10} (dose at which 10% of a population exhibits the effect) has been estimated to be 4 Gy for erythema and 14 Gy for the more serious moist desquamation (Haskin et al. 1997; Strom 2003).

Epidermis of all regions is formed with a type of stratified structure. The skin epidermis is separated from the underlying dermis by a layer of basement membrane. The maintenance of the overall cell population is accomplished by the epidermal stem cells in the basal layer, which can both self-renew over their lifespan and differentiate progressively upward to generate multiple suprabasal layers. Most cells in the first suprabasal layer are capable of dividing, like the cells in the basal layer, and are radiosensitive. The non-dividing cells in the upper layers are transcriptionally active but gradually lose cytoplasmic organelles and transit to the outmost stratum corneum, which are essentially dead cells cross-linked by transglutaminase (Fuchs and Horsley 2008). Though as thin as only several layers of cells (about 40-60 μm), these radio-resistant cells can significantly reduce the radiation dose across the epidermis, especially for radiation with a high β-ray component (Fliedner et al. 2001). Investigations indicate that the homeostasis and radiation response of the epidermis are delicately controlled by the proliferation kinetics of various types of cells as well as the spatial organization of the tissue (Archambeau et al. 1979; Hu and Cucinotta 2014).

During spaceflight, the skin may receive a dose that is up to a magnitude greater than that received by internal organs from an SPE during an EVA when minimal protection is available (Kim et al., 2006a). Risks of concern include erythema, moist desquamation, and epilation (NCRP 1989). The ED_{10} has been estimated to be 4 Gy for erythema and 14 Gy for the more serious moist desquamation (Strom 2003; Haskin et al. 1997). Protraction of the exposure increases the dose that is required for a given degree of severity by a factor of about 3. The response of the skin depends on

the number of exposures, the total dose, the dose per exposure, and the volume of tissue that is irradiated (Turesson and Notter 1984). It has been noted that deterministic radiogenic skin injury complicates the treatment of many of the high-dose casualties at Chernobyl (Strom 2003). Skin doses during an SPE can vary more than five-fold for different regions of the skin due to the steep dose gradients that are found in the solar proton energy spectra (Kim et al. 2006a).

c. Gastrointestinal Syndrome

The gastrointestinal (GI) system performs many integrated functions, such as absorption of fluid and electrolytes, breakdown and absorption of nutrients, and excretion of normal and toxic metabolites. The radiosensitivity of this system comes from the epithelial cell lining, which is present throughout the entire gastrointestinal tract. These cells undergo constant renewal that requires rapid cell turnover. They are thus dependent on the functionality of a pluripotent stem cell population localized in the crypts of Lieberkuhn. Exposure to high doses of radiation (> 4 Gy) results in the loss of these intestinal crypts and breakdown of the mucosal barrier (Wasalenko et al. 2004).

Early gastrointestinal symptoms include nausea, vomiting, anorexia, and diarrhea, which may occur within hours after exposure. Nausea and vomiting may stem from effects on the periphery and subsequent stimulation of higher nervous centers or from a response of the CNS. However, if these symptoms occur during the first few hours after exposure, the role of the central/peripheral nervous system is probably predominant. This is also true for the early onset of diarrhea. Early nausea and vomiting are signs of severe exposure, and early diarrhea indicates very severe damage that usually leads to death (Conklin and Walker 1987).

The late symptoms of gastrointestinal syndrome include abdominal cramps and diarrhea, which appear 1-2 weeks after exposure. All symptoms relate to a major loss of the stem cell population in the crypts and subsequent lack of ability to repopulate and to maintain the epithelial barrier (Fliedner et al. 2001). The occurrence of profuse and/or bloody diarrhea is linked to the denudation of the GI mucosa as well as to thrombocytopenia due to the impairment of the hematopoietic system (see above). This results in increased loss of fluid and electrolytes and possible entry and action of enteric (pathogenic and non-pathogenic) bacteria, thus leading to infection, dehydration, and electrolyte imbalances that are life-threatening.

d. Neurovascular or CNS Syndrome

Even though the CNS is generally considered to be composed of radioresistant tissue, exposure to moderate or high doses of radiation can result in a neurovascular syndrome. The CNS has higher regulatory control mechanisms, which have been shown to be functionally radioresponsive. Abnormal electroencephalograms have been reported following exposure to low-dose radiation, indicating the disturbance of brain activity (Gangloff 1964). Some symptoms occur almost immediately after exposure and include severe nausea, vomiting, diarrhea, disorientation, and ataxia. Within hours following the prodromal period, other symptoms may manifest, including headaches, hypotension, and fever; within weeks, neurological and cognitive deficits may become evident (Fliedner et al. 2001). The underlying pathophysiology is believed to be related to cerebral edema, inflammation, and massive endothelial damage to the microcirculatory system (Fliedner et al. 2001; Goans et al. 2012). Supportive care may include antiemetics, antiseizure medications, anti-inflammatory agents, mannitol, and furosemide (Feyer et al. 2005, 2014; Goans et al. 2012).

Symptoms such as nausea, vomiting, and anorexia characterize the prodromal phase of ARS and are essential identifying signs for the triage of irradiated persons (Sine et al. 2001).

Though these clinical symptoms are expressed by the gastrointestinal system, they are physiologically controlled by the CNS (Scarantino 1994). The entire process involves key components of the CNS, including areas in the hindbrain and the abdominal vagal afferents. Areas in the hindbrain were previously thought of as a vomiting center that controls all afferent impulses that can initiate emesis (Wang and Borison 1950). The current concept regarding this coordination process is that it is controlled not via an anatomical unit but through a number of loosely organized areas within the medulla, which are termed the "central pattern generator" (Hornby 2001). They generate efferent signals that are sent to relevant organs and tissues to induce vomiting after receiving a stimulus from the dorsal vagal complex located in the dorsal brain stem, which contains receptors for several neurotransmitters with potentially important roles in the emetic response. These receptors include the neurokinin-1, 5-HT3, and dopamine-2 receptors, which bind to substance P, 5-HT, and dopamine, respectively. These neurotransmitters are released from the enteroendocrine cells located in the gastrointestinal mucosal of the proximal small intestine once exposed to whole-body irradiation or large volume partial body irradiation. They bind to the appropriate receptors on the adjacent vagal fibers, leading to an afferent stimulus that terminates in the dorsal brain stem. Other sources of afferent input have also been proposed, which include the area postrema (Miller and Leslie 1994; Borison 1989) and structures in the limbic lobe, such as the amygdala (Zagon et al. 1994; Strominger et al. 1994; Horn et al. 2007).

Fatigue and weakness are also common syndromes in accident and/or radiotherapy patients, and they last much longer than the nausea and vomiting symptoms. They are known to be more distressing and can negatively affect cognitive performance, mood, and physical function (Curt 2000). There are many factors, acting independently or interactively, that are likely involved in the development of fatigue and weakness. Recent research on cancer patients and in animal experiments have led to several plausible hypotheses regarding the mechanism of radiation-induced fatigue and weakness. One hypothesis is that radiation causes an increase in brain serotonin (5-HT) levels and/or upreguation of a population of 5-HT receptors, leading to reduced somatomotor drive and working capacity (Andrews et al. 2004). 5-HT has numerous functions, including appetite control, sleep, memory, learning, temperature regulation, mood, behavior, cardiovascular function, muscle contraction, endocrine regulation, and depression. Its role in fatigue development has been verified in investigations of exercise-induced fatigue and chronic fatigue syndrome (Ryan et al. 2007). Another potential mechanism of fatigue is related to the dysfunction of the hypothalamic-pituitary-adrenal (HPA) axis. The HPA axis is the central regulatory system controlling the release of cortisol, a stress hormone that regulates blood pressure, cardiovascular function, carbohydrate metabolism, and immune function. Investigations of breast cancer survivors indicated that women who experienced fatigue had significantly lower serum cortisol levels than those who did not report fatigue (Bower et al. 2002). Alterations of the HPA axis by radiation are evident in previous studies (Schmiegelow et al. 2003). In addition to these hypotheses proposed based on clinical and animal studies, vagal afferent nerve activation, proinflammatory cytokine dysregulation, and comorbid condition (e.g., anemia, cachexia, depression, and sleep disorder) are also suspected to play roles in the development of fatigue (Ryan et al. 2007). It is generally accepted that the mechanism of radiation-induced fatigue and weakness is multifactorial and involves the dysregulation of several interrelated physiological, biochemical, and psychological systems.

3. Hereditary and Fertility Effects

NASA, in past reviews, has included the risks of hereditary, fertility, and sterility effects under the discussion of acute radiation risks. Although there is no perfect match of these effects with any of the four major radiation risks (acute, cancer, degenerative, and CNS) identified by the NASA Human Research Program, based on the past reviews of these effects (NCRP 1989a, 2000), they alone are not likely to rise to the level of a major concern. Because SPEs would be the primary cause of hereditary and fertility effects, these items are included as part of the acute category of risks.

Comprehensive reviews of the literature regarding heritable genetic risks associated with radiation exposure have been published by the United Nations Scientific Committee on the Effects of Atomic Radiation (UNSCEAR 2001) and by the Committee to Assess Health Risks from Exposure to Low Levels of Ionizing Radiation (NRC 2006). No evidence of hereditary risks has been reported from human studies, largely on the children of the victims in Hiroshima and Nagasaki (Neel et al. 1990; Nakamura 2006). However, growth retardation and other health effects have been reported in the progeny of mice exposed to radiation (Cattanach et al. 1993; Nomura et al. 2004).

For humans, mutations at specific minisatellite loci have also been investigated in the children born to parents exposed to radiation (BEIR VII 2006). These loci do not code for proteins, and changes in them are not associated with adverse health effects. Studies on the populations living in Belarus and Ukraine after the Chernobyl accident, and in the Semipalatinsk nuclear test site, have reported increased mutation rates at the loci for estimated parental gonadal doses ranging from 20 mSy to 1 Sv (Dubrova et al. 1996; Dubrova et al. 2002). However, other studies on the children of Chernobyl clean-up workers and children of A-bomb survivors failed to identify an increase in the minisatellite mutation frequency (Livshits et al. 2001; Kodaira et al. 1995). Similarly, genetic studies, including investigations of chromosome aberrations, in the offspring of A-bomb survivors indicate no effects of radiation from parental exposures (Nakamura 2006).

Exposure to space radiation may result in reduced sperm counts and changes in other semen characteristics. Human germ cells, which include sperm cells and oocytes, are sensitive to radiation. Spermatogenesis has been detected in cancer patients who received testicular doses of 0.2 - 0.8 Gy from scattering radiation (Centola et al. 1994) and in experimental rodents after radiation exposures at doses as low as 0.01 Gy (Sapp et al. 1992). A single acute exposure to low-LET radiation at testes doses of 0.5 Gy could cause temporary sterility, with recovery periods dependent on the dose (Yarbro and Perry 1985). Doses above 6 Gy may cause permanent infertility (Schover 2005; Meistrich 2013). Testicular damage has also been reported for exposures at low dose rates in animal studies (Gong et al. 2014). In a human study, direct comparison of the semen characteristics between the health workers occupationally exposed to ionization radiation and the control group revealed significant differences in motility characteristics, viability, and morphological abnormalities (Kumar et al. 2013).

Newborn girls have a finite number of about 2 million oocytes, which become reduced with increasing age (Ogilvy-Stuart and Shalet 1993). Radiation is known to damage human oocytes, with an estimated low-LET dose of 2 Gy to the ovary destroying 50% of immature oocytes (Wallace et al. 2003). Women who are older than 40 years at the time of exposure will have a smaller pool of remaining oocytes; doses in the range of 4-7 Gy for low-LET radiation may cause permanent infertility in this cohort of women from a single exposure (Ogilvy-Stuart and Shalet 1993). The estimated dose causing permanent sterility in young women exposed chronically is 20 Gy (Ogilvy-Stuart and Shalet 1993). Temporary or reduced fertility may occur at acute doses as

low as 1.25 Gy (Damewood and Grochow 1986). Limited high-LET data indicated greater effectiveness of neutrons in inducing apoptosis in the oocytes of female mice (Nitta and Hoshi 2003).

Temporary sterility for male astronauts may be the worst potential outcome if the testes receive a dose of greater than 0.5 Gy during a SPE. For female astronauts, the doses received during a large SPE may cause a reduction of the remaining oocyte number. Whether such a reduction will impact the ability to conceive after a mission will depend on the age of the astronaut at the time of radiation exposure and other factors such as the dose rate. However, doses to the ovaries are estimated to remain well below 0.3 Gy for most shielding configurations and historical SPE events (https://oltaris.larc.nasa.gov/). No human data so far have indicated an inheritance of diseases from parents exposed to low-LET radiation, and no human data are available for high-LET radiation. Preserving the germ cells prior to a space mission can reduce any potential reproductive or hereditary radiation risks in the astronauts.

B. Ground-based Studies on Acute Radiation Effects

1. RBE and Dose Rate Studies in Mice, Rats, Ferrets, and Larger Species

The data for ARS as a result of exposure to high-LET radiation, e.g., neutrons and heavy ions, are collected primarily via animal studies. As mice and rats do not display the prodromal effects such as vomiting, limited research on this particular ARS has been performed on ferrets using HZE radiation. Rabin et al. (1992, 1994) studied the dose response of 600 MeV/n ^{56}Fe ion-induced emesis in ferrets and compared it with the dose response from other radiation types. Over the dose range of 0.2 to 0.5 Gy, fission spectrum neutrons and ^{56}Fe ions were more effective than ^{60}Co gamma-rays in inducing emesis, and the effects of the ^{56}Fe ions and fission neutrons could not be distinguished from each other. ^{60}Co gamma-rays were significantly more effective in producing emesis compared with high-energy electrons or 200-MeV protons. The dose rates ranged from 0.1 to 1 Gy/min. The relatively large difference in LET between ^{56}Fe ions and fission neutrons was not associated with any difference in the effectiveness with which the two types of radiation produced emesis. As discussed above, the dose due to high-LET radiation is expected to be relatively small. More recently, animal model systems have been utilized to evaluate acute effects from exposure to SPEs including the following biological endpoints related to ARS: vomiting (and/or retching) and white blood cell counts in ferrets; white blood cell counts, fatigue, and immune system parameters in mice; and skin injury, with accompanying immune system changes and white blood cell counts in the Yucatan minipig. In addition, the effects of combined exposure to simulated microgravity and space radiation on blood cell counts and immune system functions with respect to both the innate immune system and the acquired immune system were evaluated in mice (Kennedy 2014). Research focused on characterizing the ARS response in animals exposed to SPE-like space radiation as well as the evaluation of known countermeasures for these effects.

For hematopoietic effects, significant decreases in white blood cell counts were observed in mice, ferrets, and pigs irradiated at high and low dose rates, ranging from doses of 25-50 cGy up to 2 Gy (Ware et al. 2010; Maks et al. 2011; Wilson et al. 2011; Gridley et al. 2011; Romero-Weaver et al. 2013; Sanzari et al. 2013a). However, regarding SPE radiation effects on blood cell counts, the findings in mice, ferrets, and pigs were not comparable. The RBE values were very different in the three species with respect to blood cell counts measured after animal exposure to

SPE radiation. The RBE values measured in ferrets and pigs were considerably larger than those calculated for mice (Maks et al. 2011; Sanzari et al. 2013c, 2014). For many endpoints in these studies, the RBE values increased with lower doses of SPE radiation in the dose ranges evaluated (Sanzari et al. 2013e). At doses of 25 cGy to 2 Gy of SPE proton radiation, ferrets had increased bleeding times beginning shortly after irradiation. By 13 days after receiving a dose of 2 Gy SPE proton, the ferrets had severe clotting abnormalities and many of the irradiated ferrets developed symptoms of disseminated intravascular coagulation (Krigsfeld et al. 2012, 2013a, 2013b). This is probably due to the significant decline of platelet concentrations in peripheral blood after irradiation.

For neurovascular effects such as vomiting and retching, increases were observed in ferrets irradiated at high and low dose rates, starting at doses of 75 cGy and up to 2 Gy (Sanzari et al. 2013b). Gamma-ray and proton irradiation delivered at a high dose rate of 0.5 Gy/min induced dose-dependent changes in the endpoints related to retching and vomiting. The minimum radiation doses required to induce statistically significant changes in retching- and vomiting-related endpoints were 0.75 and 1.0 Gy, respectively, and the RBE of proton radiation at the high dose rate did not significantly differ from 1. Similar but less consistent and smaller changes in the retching- and vomiting-related endpoints were observed for groups irradiated with gamma-rays and protons delivered at a low dose rate of 0.5 Gy/h. Because this low dose rate is similar to a radiation dose rate expected during a SPE, these results suggest that the risk of SPE radiation-induced vomiting is low and may reach statistical significance only when the radiation dose reaches 1 Gy or higher (Sanzari et al. 2013b).

Several studies analyzed the effects of space radiation alone and combined with modeled microgravity on immune system parameters. Alterations in the immune system related to the gastrointestinal tract were observed in mice exposed to both gamma-rays and SPE-like proton radiation. Irradiated mice exhibited breaks in the intestinal epithelial barrier that allowed the entry of bacteria and bacterial products into the circulation and their dissemination in the body (Ni et al. 2011). These effects appear to be exacerbated when combined with modeled microgravity in hindlimb-unloaded animals (Zhou et al. 2012).

In other studies performed with radiation +/- hindlimb unloading in mice, it was observed that the splenic T lymphocyte population is significantly decreased in the irradiated + HU group (compared with the non-treated control group). The results also indicated that splenic T cells that were isolated and exposed to exogenous activation in the irradiated +/- HU groups had a reduced ability to become activated (compared with the results from the HU group and the non-suspended, sham-irradiated group) (Sanzari et al. 2013d).

Acute research studies will provide critical quantitative biological data for the further development of probabilistic risk assessment tools. Extrapolation of animal results to humans is essential to quantify crew risk. The dose response relationships measured for these endpoints need to be compared mathematically with published results for human subjects to approximate the dose threshold for an equivalent response in humans in such a way that the predictive value of these animal models can be utilized to accurately assess the potential risks to humans in various adverse scenarios. Future research will emphasize the likelihood of a compromised immune system due to high skin doses from a SPE or due to synergistic space flight factors (e.g., microgravity) and the possibility of increased risk to the BFO at relevant doses, evaluating thresholds at and around the permissible limits identified in Table 1.

2. RBE and Dose Rate Studies of Cell Inactivation

Because some of the ARS effects are related to cell killing or tissue damage, the RBE and dose rate data for cell inactivation by protons can provide insight for understanding ARS resulting from SPE exposures (Cucinotta 1999; Yang 1999). Early results of cell inactivation by charged particles over a wide range of LET have been reviewed by Ainsworth (1986). In general, the RBE for cell inactivation in vitro peaked at an LET of around 100 keV/µm, and the peak RBE value varied between 1.5 and 5 for different cell types. The maximum RBE for in vivo responses tended to be lower and occurred at a lower LET value compared with the in vitro data. The reported RBE-LET relationship for in vitro cell killing showed similar trends to those of the early in vivo data (Furusawa et al. 2000).

Factors that determine the dose rate dependence of ARS include: the kinetics of DNA repair, apoptosis, cell-repopulation and proliferation, and dose distributions across critical organs. Irradiation at lower dose rates is known to reduce the probability of lethality of ARS that is induced by low-LET radiation compared with acute irradiation, as illustrated in Figure 2. Differences between dose rate effects for protons and X-rays or gamma-rays may occur due to the heterogeneous dose contribution from slowing protons or recoil nuclei for SPE organ doses. The heterogeneous dose distribution across the bone marrow for protons should lead to a sparing effect that complicates comparisons with gamma-rays (where doses are more uniform). The dose distribution across the stomach and other organs in the gastrointestinal tract also varies several-fold for SPEs, which complicates the use of gamma-ray data to predict prodromal risks from SPEs.

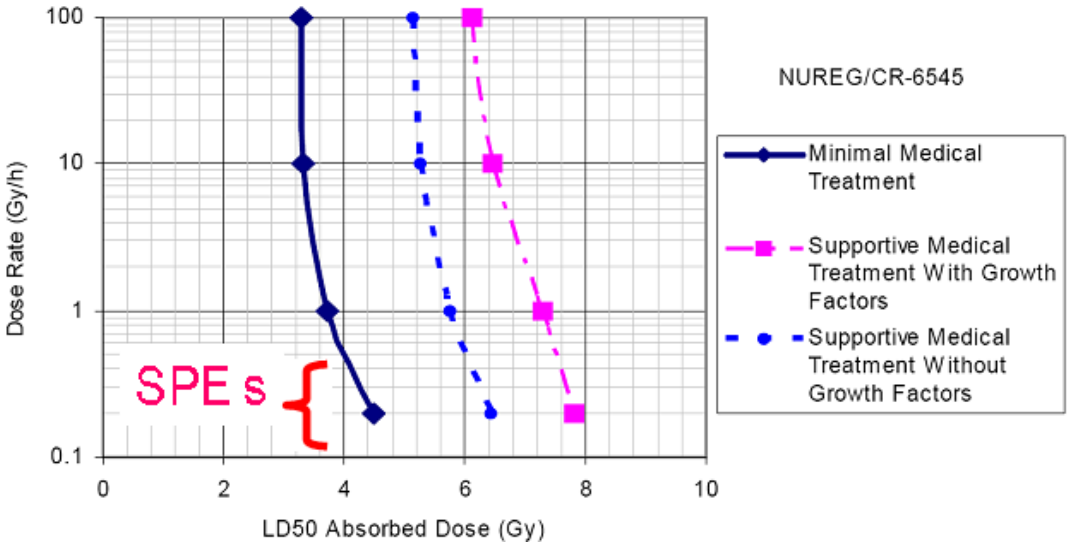

Figure 2. Effects of medical treatment and dose rate on the LD50 for gamma radiation and the expected region of dose rates for SPEs during EVA (adapted from Haskin et al. 1997).

V. Computer-Based Modeling and Simulation

The possible acute health effects to interplanetary crews from large SPEs have previously been analyzed by several researchers. To our knowledge, the first evaluation was performed with

a lethal-potentially lethal model (Curtis 1986). Another response model developed by the U.S. military for nuclear warfare (Jones 1981) was used to investigate the BFO effects after exposure of an August 1972 SPE (Wilson et al. 1997). In the following section, some recent efforts in the mathematical modeling of ARS in various systems are summarized.

A. Radiation-Induced Performance Decrement (RIPD) Models

RIPD radiobiological models were developed by the Defense Nuclear Agency in the 1980-90s (Anno et al. 1996) with the aim of providing a symptomatology basis for assessing early functional impairment of individuals who may be involved in civil defense and various military activities in the event of a nuclear attack. These models utilized six sign/symptom (S/S) categories of ARS: upper gastrointestinal distress (UG), fatigability and weakness (FW), lower gastrointestinal distress (LG), hypotension (HY), infection and bleeding (IB), and fluid loss and electrolyte imbalance (FL). In initial work (Anno et al. 1985), the severity of each of these S/S categories was described empirically as a function of absorbed dose and time-after-exposure for prompt exposures. In later work, physiologically-based models were developed (Anno et al. 1991, 1996) and incorporated into the RIPD code (Matheson et al. 1995) to estimate the S/S severities for protracted exposures. Specifically, the UG model calculates the kinetics of the production and metabolic clearing of toxins within bodily fluids, the LG model calculates the cellular kinetics of intestinal mucosa, and the FW model calculates the kinetics of lymphocytes and the resulting cytokine production. Each model employs a set of differential (rate) equations emulating relevant biological processes and containing the radiation dose and/or dose rate as a driving term causing damage and/or illness. For each model, a variable such as a toxin level or a cellular population level determines the severity of symptoms. The model equations and parameters arise from basic research in radiobiology and radiation oncology, with all models adjusted based on the best available human data.

The correlation of incidence as well as severity of various symptoms with exposed dose and dose rate was conducted by performing maximum likelihood prohibit analysis of empirical data (Anno et al. 1985). While severity is a measure of the effect on a particular individual, incidence is a population-based measure of the effect on a certain group, i.e., at some specified dose level, and incidence quantifies the proportion of individuals expected to respond according to a defined level of severity. The main body of empirical data includes effects of victims of nuclear radiation accidents and clinical accounts of cancer patients who received total body irradiation therapy from the 1940s to the 1980s. Each S/S category described above was scaled from 1 to 5 with descriptive levels of increasing severity based on medical records and common clinical practice, with Level 1 being normal and Level 5 representing the most severe state of the syndrome (Table 5) (Matheson et al. 1995). Then, a temporal response pattern for each syndrome was estimated for various ranges of prompt radiation exposure, including the onset, duration, and time-dependent severity. The protracted irradiation cases were treated similarly with consideration of sparing effects due to biological recovery that modify the level of response.

RIPD models have been applied to assess various ARS effects on astronauts if they adversely encountered the August 1972 SPE (Hu et al. 2009). The inside-spacecraft modeling starts when the calculated dose rate exceeds 0.1 cGy-eq/h, which is considered by the RIPD software as the threshold required to cause human acute effects. From the calculation of the August 1972 SPE, a male crewmember behind a typical spacecraft shielding (5.0 g/cm2) would have 24

hrs of consecutive exposure above this limit (Figure 3). The peak BFO dose rate appeared at the 7th hour from the onset of organ-sensible flux, with a value of 12.34 cGy-eq/h (Figure 3b). The upper gastrointestinal (UG) response has a maximum value of 2.0 at the 16th hour and returns to normal after the end of this period (Figure 4). The UG syndrome is quite mild and has a low expected incidence of 2% (with 95% confidence limits of 0 to 35%). According to the RIPD documentation, only sensitive personnel would exhibit stomach upset, a clammy and sweaty feeling, mouth-watering, and frequent swallowing. No vomiting would occur. A peak in fatigability and weakness (FW) severity of about 1.6 appears within a few hours after that of UG but persists and rises to a level of about 1.8 at 1000 hours. Both levels of severity indicate a rather mild FW response. The expected incidence of FW is 17% (with 95% confidence bounds of 3 to 34%). The low incidence and severity of acute effects indicate that a typical spacecraft shielding (5.0 g/cm2) is sufficient to attenuate the SPE of the historical worst case to avoid acute injury to male crews (Hu et al. 2009) without seeking shelter in a more heavily shielded storm shelter (10 to 20 g/cm2). However, the persistence of the mild FW syndrome for such a long time period should be of concern for the health of astronauts in the high-risk environment of space.

Table 5. Textual descriptions of the symptom severity level and acute radiation syndrome (adapted from Matheson et al. 1995).

Severity level	UG	LG	FW	HY	IB	FL
1	No effect	No effect	No effect	No effect	No effect	No effect
2	Upset stomach, clammy and sweaty, mouth waters	Feels uncomfortable urge to have bowel movement	Somewhat tired, with mild weakness	Slightly light-headed	Mild fever and headache	Thirsty and has dry mouth, weak and faint
3	Nauseated, considerable sweating, swallows frequently to avoid vomiting	Occasional diarrhea	Tired, with moderate weakness	Unsteady upon standing quickly	Joints ache, considerable sweating, moderate fever, no appetite, sores in mouth and throat	Very dry mouth and throat, headache, rapid heartbeat
4	Vomited once or twice, nauseated, and may vomit again	Frequent diarrhea, cramps	Very tired and weak	Faints upon standing quickly	Shakes, chills, and aches all over, difficult to stop any bleeding	Extremely dry mouth, throat, and skin, very painful headache, difficult to move, short of breath, burning skin and eyes
5	Vomited several times, including the dry heaves, severely nauseated, and will soon vomit again	Uncontrollable diarrhea and painful cramps	Exhausted, with almost no strength	In shock, breathing rapidly and shallowly, motionless, skin cold, clammy and very pale	Delirious, overwhelming infections, cannot stop any bleeding	Prostrate

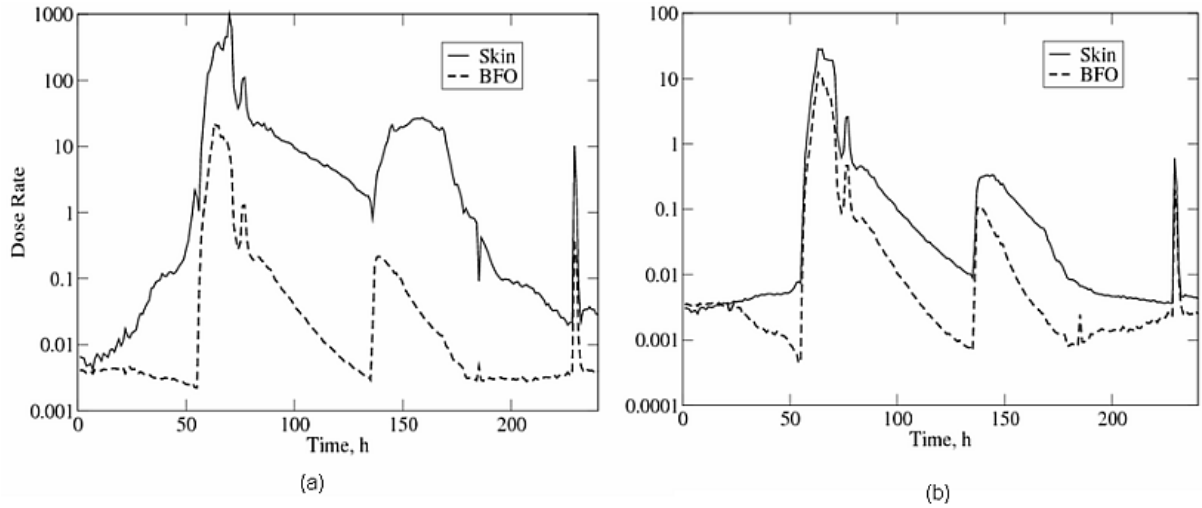

Figure 3. The skin and BFO dose rates within a spacesuit during EVA (0.3 g/cm^2) (a) and inside a spacecraft (5.0 g/cm^2) (b). The unit is cGy/h for the skin dose rate and cGy-eq/h[1] for the BFO dose rate (Hu et al. 2009).

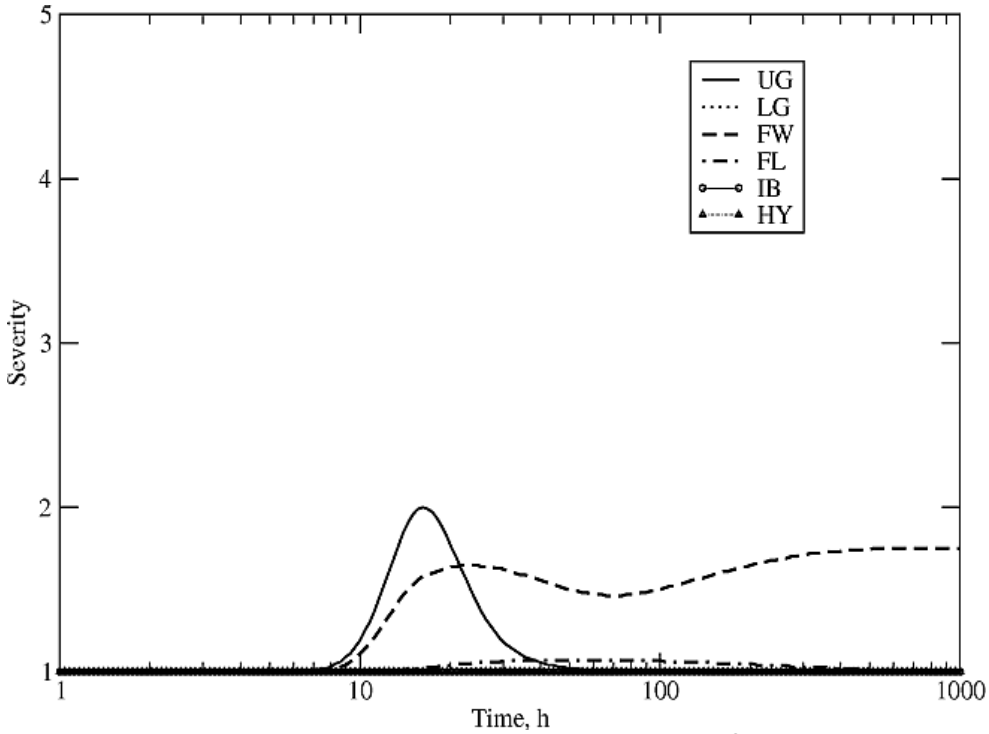

Figure 4. Acute response of male astronauts inside a spacecraft (5.0 g cm^{-2}) after the August 1972 SPE (Hu et al. 2009).

B. Hematopoietic Response Models

The radiation-induced perturbation of the hematopoietic system has been intensively investigated for several decades (Bond et al. 1965), and attempts have been made to model this complex system via biomathematical methods (Steinbach et al. 1980; Wichmann and Loeffler

1985; Fliedner et al. 1996). However, these models are built upon a very detailed architectural organization from hematopoietic stem cells (HSCs) to mature blood cells, which are speculated to comprise up to 31 stages (Dingli et al. 2007) and contain a large number of variables and coefficients that are difficult to determine experimentally. A set of coarse-grained hematopoiesis models introduced by Smirnova et al. (Zukhbaya and Smirnova 1991;Kovalev and Smirnova 1996) have been successfully utilized to simulate and interpret the experimental data derived from acute and chronic irradiation of rodents (Smirnova 1999; Smirnova and Yonezawa 2003, 2004). The models consider all four major cell lines (granulopoiesis, lymphopoiesis, erythropoiesis, and thrombopoiesis) in a framework of negative feedback control via an implicit regulation mechanism. Each cell line consists of either three or four coarse-grained compartments and explicit parameters measurable by conventional hematological and radiobiological methods (Kovalev and Smirnova 1996). Most models use several equations with explicit regulators to simplify the complicated chains of substances and reactions that are involved in the hematopoietic regulation (e.g., Fliedner et al. 1996; Wichmann and Loeffler 1985). It has been observed, however, that for each cell line, a network of hematopoietic cytokines exists that regulate cell viability, multiplication, and differentiation (Sachs 1996), and there are also nervous system factors characterized by myelinated and unmyelinated nerve fibers in bone marrow that control cellular flow. In addition, there are cellular factors such as the continuous migration of HSCs through the blood that assure a sufficient number of HSCs in each bone marrow subunit (Fliedner et al. 2002). These factors work together to allow the heterogeneously distributed bone marrow to act and react as "one organ" in the complicated cell renewal processes throughout the entire body. An implicit treatment of such a complex mechanism is superior to the explicit treatment, as the regulation events are not just local but more similar to how a system operates across all levels of organization. With this advantage and the simplified coarse-grained hematopoietic compartmental structure, effects of various radiation conditions can be easily incorporated into the cellular kinetic equations, and a dynamic relationship between the peripheral blood cells and the bone marrow precursor cells after radiation damage can be rigorously established (Kovalev and Smirnova 1996; Hu and Cucinotta 2011).

The granulopoietic model proposed by Smirnova et al. (2011) has been extended from rodents to large animals and humans (Hu and Cucinotta 2011a). By introducing species-dependent hematopoietic and radiobiological parameters, the granulopoietic model can generate results consistent with the data from experiments on beagle dogs and rhesus monkeys, as well as with acute, protracted, and chronic radiation conditions from various sources (Hu and Cucinotta 2011b). This implies that this model may provide a correct quantitative description of the hematopoietic response that covers a broad range of radiation conditions and species and could be a potential unified model with which to characterize mammalian hematopoietic responses after irradiation. By extending the model to humans, some empirical data on the hematopoietic response of victims after radiation accidents can also be reconstructed. In addition, this model can calculate the survival portion of bone marrow precursor cells after various types of exposure, which is essential for determining the likelihood of reversible or irreversible injury of the hematopoietic system (Fliedner et al. 1996). As an application in space radiation risk assessment, the model can be used to simulate the possible suppression of granulocytes in an astronaut in interplanetary space under chronic stress from low-dose irradiation, as well as the granulopoietic response if a historically large SPE is encountered (Hu and Cucinotta 2011b).

For long-duration space missions beyond low-Earth orbit, crew members will be exposed to a chronic background of high-LET GCR with the possibility of encountering a large but

infrequent SPE. Figure 5a shows the modeled granulopoietic effects under the chronic dose rate of 1.5 mSv/d, which has been predicted for the GCR dose near a solar minimum (Cucinotta et al. 2006). Though the level of granulocytes in blood is just slightly depressed, according to this model, there will be a persistent presence of weakly damaged X_1 cells in bone marrow. Figure 5b shows the simulated granulocyte modulation for an astronaut in a typical spacecraft traveling in interplanetary space if he encounters a SPE 100 days after the launch. The SPE is postulated to be the same as the historically worst-case August 2, 1972, event. At the peak of this event, the exposure in a lightly shielded spacecraft (5.0 g/cm^2) would have been about 443.0 mSv over a 10-hour increment (Hu et al. 2009), assuming that crew members do not seek shelter in a more heavily shielded storm shelter. In this example, the chronic GCR dose rates are assumed to be 1.0 mSv/d to more closely represent solar maximum conditions, as large SPEs are known to occur at different parts of the solar cycle. The granulocyte concentration in blood can be as low as 75% of the normal level shortly after the peak of an SPE. At the nadir of the granulocyte counts, the level of intact X_1 cells in bone marrow is about 35% of the normal level because most cells in this pool experience at least weak damage from the high-dose-rate irradiation. Previous studies indicate that such an adverse scenario within a short period will not cause hematopoietic failure and that the system will recover automatically (Fliedner et al. 1996; Wilson et al. 1997). However, the response of the system to additional SPEs would be weakened, a situation that is possible during long-duration space missions (Kim et al. 2009a). This scenario is the basis for the 1970 National Academy of Sciences (NAS/NRC 1970) recommendation for a 0.50 Sv/y limit for the protection of the blood system that is still currently used by NASA.

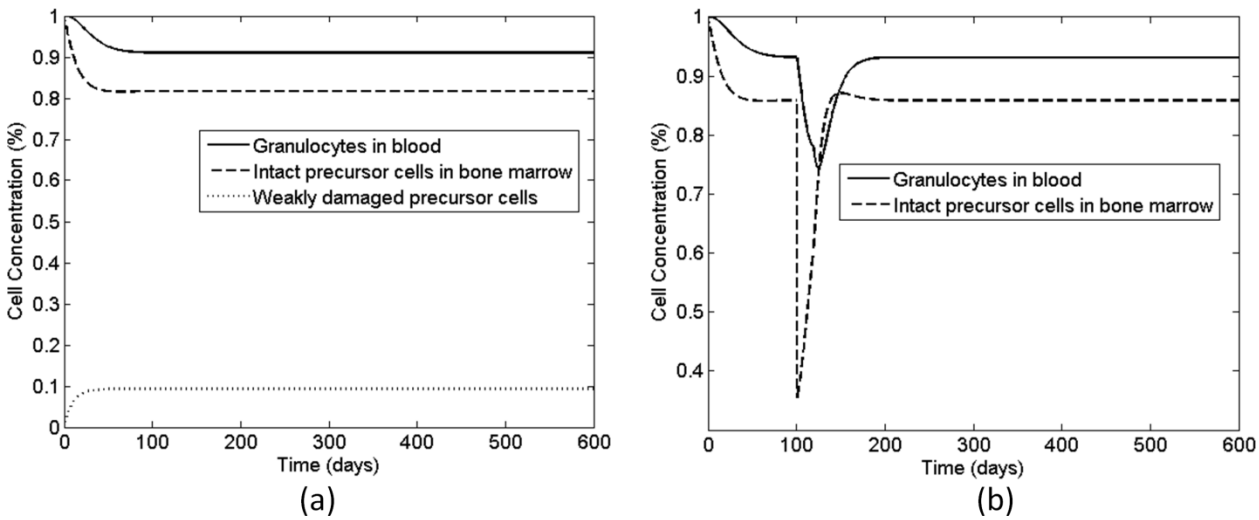

Figure 5. Granulocyte levels after space radiation exposures (Hu and Cucinotta 2011b). (a) Reduction of granulocytes under 1.5 mSv/d of continuous exposure to GCR at solar minimum. The concentrations of intact and weakly damaged X_1 cells in bone marrow are also shown. (b) Modulation of granulocyte levels and intact precursor cells if an astronaut encounters the historically worst SPE. Before and after the SPE, the dose rate of GCR is assumed to be 1.0 mSv/d.

A recent investigation indicated that the lymphopoiesis model proposed by Smirnova can also qualitatively and quantitatively describe a wide range of accidental data in vastly different

scenarios if adapted with model parameters for humans (Hu et al. 2012). The results are consistent with the two widely recognized empirical biodosimetric tools, Guskova's method and Goans' method, demonstrating the potential to use the models as an alternative method for the assessment of radiation injury. In accidental situations, the exposure may involve poorly penetrating beta radiation and very penetrating gamma-ray, X-ray, thermal, and intermediate neutron radiation (Guskova et al. 2001). Thus, most individuals involved in accidents received non-uniform irradiation rather than uniform whole-body irradiation. Biodosimetric markers, such as persistent lymphopenia or the cytogenetic assay, are particularly important for assessing whole-body damage, as they reflect the average response required to cope with the injuries at various levels of the physiological system (Guskova et al. 2001). They also provide more accurate information for medical decision-making than physical detection devices (Dainiak 2002). The lymphopoiesis model is therefore very useful for interpreting biodosimetric marker data following accidental radiation exposures (Hu et al. 2012).

Thrombopoietic and erythropoietic models have also been extended to describe human hematopoietic responses after acute radiation or during chronic radiation exposures (Smirnova 2012). In essence, all hematopoietic cell renewal systems have a very similar structure and function (Fliedner et al. 2002). The hematopoiesis models proposed by Smirnova et al. (2009) describe the mechanism of blood cell production starting from the pluripotent stem cell through different development stages, represented by the coarse-grained compartments, and the degree of cellular loss quantified by the radiosensitivity parameters of each compartment as well as the absorbed doses. The underlying implicit regulation mechanisms reflect the features of a systems-level response of the hematopoietic system to exogenous perturbations, which is reflective of the fact that the bone marrow, though heterogeneously distributed throughout the skeleton, acts as one organ of blood cell renewal for the whole body. Such a scheme seems to be applicable to all hematopoietic cell lineages and different radiation conditions (Hu et al. 2012; Hu and Cucinotta 2013); thus, it is possible to develop a unified model to characterize mammalian hematopoietic responses after irradiation, which has been pursued by many researchers for several decades (Bond et al. 1965; Fliedner et al. 2007).

C. Epidermal Response Models

It is interesting that such a scheme can also be applied to simulate the cellular alterations observed in the patches of skin epidermis exposed to high-dose acute irradiation (Smirnova et al. 2014). In this model, the epidermal keratinocytes are separated into three groups according to the degree of their maturity and differentiation:

- X: the dividing maturing cells of the basal layer (from stem cells to mature basal cells);
- Y: the maturing cells of the joint spinous/granular layer (from spinous cells to granular cells, i.e., prickle cells);
- Z: the cells of the corneal layer (corneal cells or squames).

The dynamics of the skin epidermal epithelium are represented by a system of ordinary differential equations, which resemble those used in the models of major hematopoietic lineages discussed above. With cell kinetics parameters experimentally determined in swine epidermis, the modeling results for the dose- and time-dependent changes in basal and prickle cell populations are in good agreement with relevant experimental data. In addition, the simulations also reveal that a correlation exists between the dynamics of a moist reaction experimentally observed and the corresponding in silico dynamics of corneal cells. From this information, the threshold level of

corneal cells (which indicates the appearance of the moist reaction) can be identified (Smirnova et al. 2014).

A different approach using a multiscale soft tissue framework can also be employed to simulate the skin epidermal homeostasis and radiation responses (Hu and Cucinotta 2014). The model couples the following fundamental processes:

- Subcellular level: Wnt signaling, cell-cell adhesion, and cell-cycle control;
- Cellular level: Cell division, migration, and differentiation;
- Macroscale level: Extracellular Wnt profile, cell-cell adhesion, and basal cell-BM adhesion.

The connections between cells are modeled as springs, and Voronoi tessellation is used to associate the cell centers and to determine the size and shape of every cell in the aggregate. The cell-cycle progression, cell-cell adhesion, and differentiation states are influenced by intra-, inter-, and extracellular cues. By incorporating experimentally measured histological and cell kinetic parameters in this well-developed multiscale tissue framework, population kinetics and proliferation index results comparable to observations in unirradiated and acutely irradiated swine experiments can be obtained (Hu and Cucinotta 2014). Based on the simulation results, it can be demonstrated that a moderate increase in the proliferation rate of the surviving proliferative cells is sufficient to fully repopulate the area denuded by high doses of radiation, as long as the integrity of the underlying basement membrane is maintained. The importance of considering proliferation kinetics as well as the spatial organization of tissues during in vivo investigations of radiation responses is also highlighted.

The epidermis of swine is known as the closest to that of humans in terms of structure, histology, and cell kinetics. Nevertheless, extrapolation of the developed models to humans needs further investigation, as some subtle differences between the epidermis of swine and human are known even from early studies (Montagna and Yun 1964).

VI. Risk in Context of Exploration Mission Operational Scenarios

A. Cumulative Probability of a Solar Particle Event Occurrence during a Given Mission Period

Estimates of likely SPE cumulative doses and dose rates at critical organs are important for assessing the probability of ARS for specific mission scenarios. Detailed spectra and temporal information are available for most of the SPEs that have occurred since 1955. An analysis of nitrate concentrations in Arctic ice core samples provided data on integral fluences that are above 30 MeV for SPEs dating back to the 15th century (McKracken et al. 2001). However, recent work by Schrijver et al. (2012) has shown that the statistics of nitrates cannot be used as a proxy for the statistics of SPEs. Therefore, ice core data should not be used either for frequency analysis or to set upper limits of events. The use of nitrates as a proxy for SPEs should be removed from current analysis tools and not used in future work. Other proxies, such as lunar and terrestrial radionuclides, may be of use in constraining the upper limit of SPE fluences (Schrijver et al. 2012). Recent work by Kovaltsov and Usoskin (2014) revealed that an SPE with energy > 30 MeV and proton fluence > 10^{11} (protons/cm^2 per year) is not expected on mega-year timescales based on lunar radionuclide data.

For recent solar cycles 19 through 21 (1955–1986), a list of major SPEs and associated proton fluences has been assembled by Shea and Smart (1990), who placed all of the available flux

and fluence data in a useful continuous database. From 1986 to the present (solar cycles 22 and 24), both an SPE list and the Geostationary Operational Environmental Satellite (GOES) spacecraft measurements of the 5-minute-average integral proton flux can be obtained through direct access to the National Oceanographic and Atmospheric Agency (NOAA) National Geophysical Data Center. Work was done by Xapsos et al. (2004) to utilize data from the Goddard Medium Energy (GME) instrument on board the Interplanetary Monitory Platform 8 (IMP-8) satellite along with the GOES series in a consistent manner. The GOES data were calibrated to the IMP-8 data and re-binned to the finer energy bins of the GME instrument. This provides a consistent dataset from 1973 through 2006. The SPEs identified during solar cycles 19–23 varied significantly in the overall distribution of Φ_{30} from cycle to cycle. However, fluence data of Φ_{30} were combined over all 5 cycles to estimate an overall probability distribution of an average cycle.

While the expected frequency of SPEs is strongly influenced by the phase of the solar activity cycle, the SPE occurrences themselves are random in nature. The onset dates of a total of 370 SPEs during solar cycles 19–23 are marked in the top of Figure 6 as brown vertical lines. More frequent SPE occurrences are shown as dense vertical lines, which are located typically near the middle of cycles. Large SPEs with proton fluences at energies > 30 MeV, $F_{30} > 1\times10^7$ protons/cm^2 are also shown. Other than a general increase in SPE occurrence with increased solar activity, recent solar cycles have yielded no recognizable pattern of when and how large individual SPEs occur (Goswami et al. 1988; Kim et al. 2005, 2009b, 2011). There have been several occurrences of intense SPEs during solar active years, which are typically 2.5 years before and 4.5 years after solar maximum. The data in Figure 6 lead to the observation that individual SPE size is randomly distributed. This sporadic behavior of SPE occurrence and event size is a major operational problem in planning for missions to the moon and Mars.

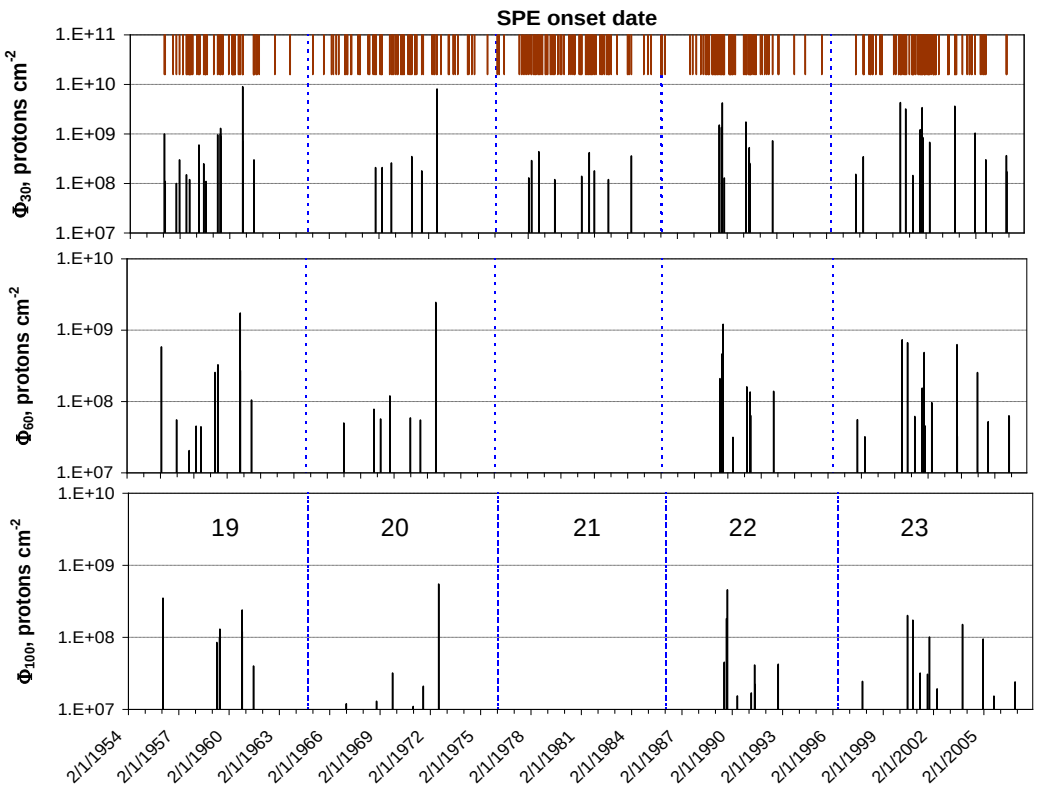

Figure 6. SPE onset date marked as vertical lines in the top of the figure, and large SPEs recorded during 5 modern solar cycles with integral proton fluences of F_{30}, F_{60}, and $F_{100} > 1\times10^7$ protons/cm^2 with energies > 30, > 60, and > 100 MeV, respectively (Kim et al. 2011).

To address the random nature of SPE occurrences and event sizes, a probabilistic approach to modeling has been the method that is often used, starting with the work of King (1974). In addition, the NASA JPL proton fluence model (Feynman 2002), the Moscow State University probabilistic SPE model (Nymmik 1999), and the Emission of Solar Proton (ESP) model (Xapsos 1999, 2000, 2007) have used similar methods to those of King. The ESA SEPEM model (Jiggens 2012) uses a virtual timeline methodology. All of these efforts utilize historical measurements, as available, and provide a cumulative SPE spectrum at some confidence level. This work is useful for mission design, as a range of confidence levels can be considered during the design phase. The work of Kim et al. (2009a) incorporates the probabilistic modeling framework but builds the probabilities from historical mathematical models of large SPE spectra.

B. Spectral Representation of Solar Particle Events

The shapes of the energy spectra, as well as the total fluence, vary considerably from event to event. Accurate organ dose estimates and particle spectra models are needed to ensure astronauts stay below radiation limits and to support the goal of narrowing the uncertainties in risk projections (Cucinotta et al. 2010). For the radiation dose assessments of astronauts from SPEs, spectral forms of incident particles extending to a few GeV have been fitted with available measurements up to ~100 MeV. Those functional forms, an exponential in rigidity (Schaefer 1957;Freier and Webber, 1963;King 1974) and a nonlinear regression of Weibull (Xapsos et al. 2000;Kim et al. 2009b), are simple and useful representations of the spectrum of SPEs; however, the spectral assumption

beyond ~500 MeV may result in the systematic uncertainty in radiation dose assessments of astronauts. With currently available assets, the energy spectrum of SPEs is only accurate up to approximately 500 MeV. Further constraint of the high-energy tail of the spectrum requires additional information not previously available from space assets. PAMELA (Adriani et al. 2015) provides direct measurements of the high-energy tail, but the measurements are limited due to its location in LEO. Ground-based neutron monitors, however, can also help provide constraints for the high-energy tail of the SPE spectrum.

A simplified technique for analyzing data from the world-wide neutron monitor (NM) network has been developed by Tylka and Dietrich (2009). They derived absolutely-normalized event-integrated proton spectra from the ground-level enhanced (GLE) event database. In this method, the fluences were extracted for individual NM stations with the quantification of the internal consistency of the results. The combined satellite and NM data from ~10 MeV to ~10 GeV from major SPEs (Tylka and Dietrich 2009) were presented as a double power law in rigidity, a so-called Band function (Band et al., 1993):

$$\Phi(>R) = J_0 R^{-\gamma_1} e^{-R/R_0} \qquad \text{for } R \le (\gamma_2 - \gamma_1) R_0$$

$$\Phi(>R) = J_0 R^{-\gamma_2} \left\{ \left[(\gamma_2 - \gamma_1) R_0 \right]^{(\gamma_2 - \gamma_1)} e^{(\gamma_1 - \gamma_2)} \right\} \qquad \text{for } R \ge (\gamma_2 - \gamma_1) R_0$$

where R in GV, E in MeV, and γ_1 and γ_2 are the spectral indexes.

Several large SPEs with GLEs recorded by neutron monitors are the events on 23 February 1956, 12-15 November 1960, 29 September 1989, 4-7 August 1972, and 19-24 October 1989. Their event-integrated differential spectra have been compared for three different functional forms using different spectral representations of large SPEs. Variations of exposure levels were compared as an approach to the development of improved radiation protection for astronauts, as well as the optimization of mission planning and shielding for future space missions.

The question of how to handle the extrapolation of SPEs at Earth to Mars and beyond is ongoing. Specifically, the radial dependence of SPEs and how to extrapolate particle fluences beyond 1 astronomical unit (AU) (1 AU ≈ 1.5×10^8 km) were investigated by Smart and Shea (2003). Smart and Shea found that the radial dependence of the SPE flux had a range from R^{-2} *(for* $R < 1$ *AU)* to R^{-4} (for $R > 1$ AU), where R is the radial heliospheric distance. Recent modeling work (Aran et al. 2005; Kozarev et al. 2010; Verkhoglyadova et al. 2012) and observations (Lario et al. 2006) revealed that the power law index values can vary significantly from the findings of Smart and Shea (2003). Some variables identified as affecting the variation in the power index include the particle energy range studied and coronal mass ejection shock obliquity and shock speed (Aran et al. 2005; Kozarev et al. 2010; Verkhoglyadova et al. 2012).

C. Temporal Profiles of Solar Particle Events

During a large SPE, there is a sudden increase in proton flux, especially for particles with energies greater than 50 MeV. The time profile of an individual SPE can be very complex due to the complicated acceleration mechanisms driving the SPE. Some SPEs can exhibit a sharp onset of high-energy protons after the major pulse (Reames 1999). While the fluence during this secondary onset may not be as large as that during the peak, the sudden increase in dose rate is an

open question with important implications for acute responses to SPEs due to the dose-rate dependence (NCRP 2000).

Total fluence of an SPE is the representative indicator of a large SPE. The detailed energy spectra for a large SPE, especially at high energies, is the most important parameter for assessing the risk of radiation exposure (Kim et al. 2006; Schwadron et al. 2010), and dose rate-dependent factors are important for assessing biological acute responses (NCRP 2000). A detailed temporal analysis of dose rate at the BFO for each SPE shows the highest dose rate at its peak, at which point significant biological damage would occur in a crew if adequate shielding is not provided (Hu et al. 2009). Early biological effects are expected to increase significantly for dose rates above 0.05 Gy/h. For an extended EVA, the current recommended 30-day exposure limit for the BFOs, which is 0.25 Gy-Eq (NCRP 2000), is easily exceeded without sufficient shelter.

A simplified model of SPE temporal variation that includes an exponential rise to a peak intensity followed by a slow decay to background levels is often used as input to obtain dose and dose rate information of interest for modeling acute radiation risk (ARR). According to the temporal evolution of Φ_{30} with the assumption of the same spectral shape of each SPE at each time step, the dose rate distribution is estimated from the total SPE exposure. The early radiation risks are assessed from the BFO dose and dose rate by using the probabilistic biomathematical models of ARR (Anno et al. 1996; Hu et al. 2009;Hu and Cucinotta 2011;Hu et al. 2012), which include lymphocyte depression, granulocyte modulation, fatigue and weakness syndrome, and upper gastrointestinal distress. The temporal profiles of severities of the relevant symptoms are simulated, and the incidence rate of individuals is estimated at the 95% confidence interval.

D. Shielding Material and Shielding Distribution of Spacecraft

The early effects from acute exposure may not be avoided when only a conventional amount of spacecraft material is provided to protect the BFO from a large SPE. To avoid placing unrealistic mass on a space vehicle while at the same time increasing safety levels for the astronauts, one solution for shielding against SPEs is to select optimal materials for the vehicle structure and shielding. To this end, it has been shown that materials that have lower atomic mass constituents have better shielding effectiveness (Wilson et al. 1999; Cucinotta 1999). Overall exposure levels from large SPEs that have been recorded in the modern era can be reduced to below 0.1 Sv when heavily shielded “storm shelters” are added to a typical spacecraft (Kim et al. 2006). Interpretation of this result, however, should be made while keeping in mind the caveat that significant uncertainties are inherent in determining the source spectra of protons (Musgrave et al. 2009).

In the development of an integrated strategy to provide astronauts maximal radiation protection with consideration of the mass constraints of space missions, the detailed variation of radiation shielding properties (Kim et al. 2010;Walker et al. 2013) is considered to improve exposure risk estimations. For shielding analysis at a specific location in the spacecraft, shielding distributions can be evaluated. Currently, ARS due to SPEs can be assessed using the ARRBOD (Kim et al. 2010) and OLTARIS (Singleterry et al. 2010) models, which incorporate the shielding distributions of various spacecraft, including the conceptual lunar/Mars/NEA transfer capsule, lunar habitat, command module of Apollo, various locations within MIR (Badhwar et al. 2002), locations of the six passive radiation dosimeters of Shuttle (Atwell et al. 1987), and the six radiation area monitors of the International Space Station (Wilson et al. 2006). OLTARIS allows

users to upload their own thickness distributions utilizing user-defined material properties for assessment and optimization.

In addition, optimization of storm shelters has been considered. Walker et al. (2013) and Simon et al. (2013) recently analyzed a trade space of different shield design concepts, including storm shelter placement within the vehicle, for multiple historic SPE spectra. The metric for shielding effectiveness in these studies was the reduction in effective radiation dose relative to the dose derived from nominal shielding conditions.

E. Solar Alert and Monitoring

An effective operational procedure requires an SPE warning or alert system. This system, which would be activated at the onset of proton exposure, would include pertinent information concerning the event, such as the fluence or flux and the energy distribution. These capabilities do not currently exist, and forecasts from NOAA are limited. New capabilities for deep space mission forecasting will be needed prior to a Mars mission because the alignment of the Earth and Mars does not allow all SPEs on Mars to be observed from Earth. A report by the NRC discussed research approaches in space science that should lead to improved forecasting and alert capabilities for SPEs (NAS/NRC 2006), including a status of approaches supported by the NASA Science Mission Directorate.

The most likely outcome of an SPE is mission disruption, with little or no harm to the crew, because despite the occurrence of some very large SPEs (e.g., the 1972 event described previously), more than 90% of SPEs result in very small radiation doses to critical organs (<100 mGy-Eq) (Kim et al. 2011). The other 10% of events can yield biologically significant doses and dose rates and are a concern for astronaut health and, therefore, mission planning.

Still, mission disruption is possible because the size of the SPE cannot be determined until several hours after its initial onset. Reliable radiation dosimeters that can transmit information to mission control and provide a self-alert to astronauts are required. Such instrumentation has been available for many years, including during the Apollo missions (NCRP 1989a). In 2009, a workshop was held to determine operational requirements for forecasting as well as the state of forecasting capability (Fry et al. 2010). The workshop concluded that models were sufficiently mature to begin assessing them against operational requirements and that there would be benefit from future research. Since the workshop, further research has been performed to improve dose forecasting using regression techniques (Moussa and Townsend 2014). Additionally, a statistical method to evaluate forecasting performance using five different metrics was developed and applied to four different forecasting models (Falconer et al. 2014).

F. Acute Radiation Risk and BRYNTRN (Baryon Transport) Organ Dose Projection (ARRBOD)

The Acute Radiation Risk and BRYNTRN Organ Dose (ARRBOD) projection code has been developed as a NASA tool to evaluate acute risks and organ doses from SPE exposures. ARRBOD (Kim et al. 2010), which includes the baryon transport code of BRYNTRN (Cucinotta et al. 1994;Wilson et al. 1989) and an output data processing code of SUMDOSE, is used to estimate the whole-body effective dose for astronauts. The radiation shielding by body tissue at specific organ sites is accounted for by using ray tracing in the human phantom models of the Computerized Anatomical Male (CAM) model (Kase et al. 1970; Billings and Yucker 1973) and

the Computerized Anatomical Female (CAF) model (Yucker and Hudston 1990; Yucker 1992). By implementing the NCRP's recommended RBE (NCRP 2000) and the full definition of neutron RBE suggested by Wilson et al. (2002), the dosimetric quantities of various organs in gray-equivalents (Gy-Eq) are calculated for male and female astronauts in case they encounter historically intense SPEs during transition and on the surface during lunar or Mars missions. The resultant organ doses for skin, eye, and BFO are compared with the current 30-day PELs (Table 1). The severity of possible ARS is assessed from the BFO dose by using the NASA-developed probabilistic model ARRBOD (Anno et al. 1996; Hu et al. 2009).

For SPE environments, ARRBOD uses the exponential spectrum and Weibull distribution function. These two functional forms can fit available satellite measurements up to ~100 MeV. The recent analysis of the SPE spectrum of the Band function is included, which fits the combined satellite and neutron monitor data to improve the spectral fits from ~10 MeV to ~10 GeV (Tylka and Dietrich 2009). In addition, as the overall probability distribution of SPE fluence for an average cycle is estimated from the proton fluence data with energy greater than 30 MeV (F_{30}) for cycles 19-23 (Kim et al. 2009a), a probability level of proton fluence can be specified by the user to analyze the exposure from SPEs. This is because the overall distribution of F_{30} is statistically significantly different from cycle to cycle in the recorded SPE data. To simulate the protracted effects of radiation exposure from SPEs, a simple representative temporal profile of SPE is modeled for the particle flux evolution by using a pulse function, which is parameterized by two time constants (the rise and decay times) and the ratio of proton flux for energies greater than 30 MeV at the peak to the onset.

With the temporal profile of the SPE described, both the temporal profile of the BFO dose rate within the spacecraft and the temporal profile of the EVA BFO dose rate can be generated for male and female astronauts. Once IVA and EVA timelines are established, the acute health response information of lymphocyte depression, granulocyte modulation, fatigue and weakness syndrome, and upper gastrointestinal distress is generated by NASA-developed prodromal risk models and hematopoietic models (Hu et al. 2009;Hu and Cucinotta 2011a, 2011b;Hu et al. 2012).

G. Potential for Biological Countermeasures

Radiation countermeasures can include radioprotectors, mitigators, and treatments. Radioprotectors, such as antioxidants, are agents that are given prior to exposure to reduce the damage to various organs by radiation (Gudkow and Komarova 2005), while mitigators are agents given during or shortly after exposure (Stone et al. 2004; Bourgier et al. 2012). Biological countermeasures under development for use in clinical practice and against radiological threats are expected to provide risk reduction for low-LET radiation delivered at high doses and dose rates. However, their effectiveness at low dose rates and for high-LET solar particle radiation is less clear and may be distinct from the countermeasures required for the other space radiation risks of cancer, central nervous system, and degenerative tissue effects. The likelihood that an SPE will produce doses that are above 1 Gy is small, but the occurrence of doses that can induce prodromal risks is possible. Although the prodromal syndrome, including nausea, vomiting, anorexia, and diarrhea, may seem more innocuous than the other symptoms of ARS, biological countermeasures for the prodromal risks are a major consideration. Ondansetron (Zofran®), a 5-HT3 serotonin antagonist, is a biological countermeasure that has been tested in animal models under space-relevant doses and dose rates (King et al. 1999) and is approved clinically for the treatment of nausea associated with radiotherapy. Ondansetron has demonstrated effectiveness in reducing

emetic risk due to space-relevant ionizing radiation and is currently used on the ISS for nausea and vomiting (Kennedy 2014). Oral anti-diarrheal agents are included in the ISS medical kit to ameliorate symptoms associated with diarrhea. While the risk of infection is another factor that requires attention, current medical kits include a range of antibiotics, namely, penicillins, cephalosporins, and macrolides (Marshburn 2008), that will be available to support a weakened immune system. These treatments have been successfully delivered orally or via intramuscular injection on previous space missions.

Following the prodromal phase, there is concern for the occurrence of hematopoietic syndrome at the anticipated exposure doses given the potential for the bone marrow to be compromised at doses as low as 0.5 Gy (Mettler 2012). There are several mechanisms being targeted for the development of radiation countermeasures to address hematopoietic syndrome, including the scavenging of free radicals, blocking cell death signals, facilitating repair of damaged molecules, and inducing regeneration of injured tissue (Whitnall 2012). A summary of several radioprotectors and mitigators that have been explored to treat hematopoietic syndrome and their various stages of development are outlined in Table 6. One of the more successful radiation mitigators, filgrastim (Neupogen®, Amgen), is a granulocyte colony stimulating factor that has shown promise in several studies when administered post-exposure and is currently part of the US National Strategic Stockpile (Xiao and Whitnall 2009; Farese et al. 2013). Neupogen® received FDA approval in 2015 for the additional indication to "increase survival in patients acutely exposed to myelosuppressive doses of radiation" (FDA 2015). The recommended dosage for patients acutely exposed to myelosuppressive doses of radiation is 10 mcg/kg/day by subcutaneous injection (Amgen 2015). The sustained release version, pegfilgastrim (Neulasta®), reduced neutropenia in studies involving SPE-like protons (Romero-Weaver et al. 2013) and has recently received FDA approval (FDA 2015) for the same indication as Neupogen® with a recommended dosage of 0.1mg/kg subcutaneously once per week for two weeks. An automated subcutaneous delivery system was recently released by Amgen to facilitate delivery of Neupogen® and Neulasta®. Antioxidants have also been investigated both *in vitro* and *in vivo* for their protective properties against radiation-induced oxidative stress, with several demonstrating promising results in SPE-relevant studies (Kennedy and Wan 2011;Kennedy 2014), and beta androstendediol administered post-irradiation had beneficial effects following heavy ion particle irradiation (Loria et al. 2011).

The anticipated SPE exposure dose to the skin ranges from 0.5-5 Gy. At the higher doses, there is an increased likelihood of radiation dermatitis, which can result in irritation, pain, and skin infections that may ultimately compromise the immune system (Peebles et al. 2012; Ryan 2012). In studies involving minipigs exposed to 5 or 10 Gy of SPE-like protons, topical steroid cream (Elocon®) mitigated radiation-induced skin damage (Kennedy 2014). Radiation exposure to skin is currently treated as a burn. Medical kits provided on the ISS include silver sulfadiazine, sterile gauze, parenteral opioid analgesics, and crystalloid solutions (Marshburn 2008), although more advanced radioprotectors and mitigators may be required for longer duration missions. These may include targeted gene therapy with targets focused on the TGFβ1 pathway inhibitor, synthetic superoxide dismutase/catalase mimetics, recombinant IL-12, toll-like receptor-5 antagonist, and inhibitors of cyclin-dependent kinases (Ryan 2012).

There are several biological radiation countermeasures currently available or under development that can be investigated to determine their efficacy in treating ARS due to SPEs. Several new therapies are also being explored, many of which are already in early-stage clinical trials, to evaluate their toxicity and safety as space radiation countermeasures. Mechanistic studies

of possible biochemical routes for countermeasure actions must be combined with approaches to extrapolate model system results to humans for such countermeasures to be used operationally by NASA. It will be important moving forward to bear in mind that the efficacy of any biological countermeasure will need to be determined under the appropriate dose and space radiation environment, and the impact on other risk areas must be considered. Selecting effective radioprotectors or mitigators will also involve practical concerns, such as ease of administration, effectiveness period, impact on performance, side effects, toxicity, shelf-life, and drug interactions, all of which will be factored into the adoption of any biological countermeasure. Continued surveillance of new technologies and radioprotectors/mitigators will guide the identification and validation of appropriate biological countermeasures for long-duration space missions.

Table 6. Summary of Biological Countermeasures Investigated for Radioprotection or Mitigation

Radiation Countermeasures for Hematopoietic Syndrome

Countermeasure	Class	Group	Mechanism	Testing	Status	References
Neupogen	Radiomitigator	Recombinant growth factor	Granulocyte Colony Stimulating Factor (G-CSF)	Rhesus macaques exposed to 7.5 Gy TBI gamma; delivery 1 and 8 days post-IR; increased survival and neutrophil-related parameters	FDA approval under Animal Rule	Xiao 2009, Farese 2013, 2014
Neulasta (pegylated form of Neupgen)	Radiomitigator	Pegylated growth factor	Granulocyte Colony Stimulating Factor (G-CSF)	Rhesus macaques exposed to 7.5 Gy TBI gamma; delivery 1 and 8 days post-IR; increased survival and neutrophil-related parameters	NHP studies conducted for FDA approval under Animal Rule	Hankey 2015
Sargramostim (Leukine)	Radiomitigator	Recombinant growth factor	Granulocyte Colony Stimulating Factor (G-CSF)	Rhesus macaques exposed to 7 Gy TBI ^{60}Co; delivery 1x/day for 23 days post-IR; Recovery from severe neutropenia	FDA approval for off-label use; included in SNS	Gupta 2013 – FDA briefing package
Amifostine (Ethyol) or WR-1065, WR-2721, WR-151,327	Radioprotector	Aminothiol	Antioxidant; free radical scavenger; DNA protector	B6CF1 exposed to 2 or 4 Gy TBI Co-60; B6CF1 exposed to 0.1 or 0.4 Gy TBI fission neutrons; delivery 30 min pre-IR; increased survival; protected against specific tumors; protected against non-tumor complications; induces adaptive response	FDA approval for renal toxicity and xerostemia in patients being treated for cancer	Peebles 2012, Soref 2011, Langell 2008, Xiao 2009, Paunesku 2008, Grdina 2013, Bogo 1985
PrC-210	Radioprotector	aminothiol	Antioxidant; free radical scavenger; DNA protector	ICR mice exposed to 8.63-8.75 Gy TBI ^{137}Cs; delivery 30 min pre-IR; increased survival	Testing ongoing at AFRRI	Copp 2013
B-190 (Indralin)	Radioprotector	alpha1-adrenergic receptor	Vasoconstrictor; neutralizes the oxygen effect	Rhesus macaques exposed to 6.8 Gy TBI ^{60}Co; delivery 5 min pre-IR; antimicrobials post-IR: levomycetin 1x/day for days 1-10 and pen/strep combination 1x/day for days 10-20; increased survival	Testing ongoing in Russia	Vasin 2014

Androstenediol (5-AED)	Radioprotector and mitigator	Steroid	Nuclear Factor-κβ; increases G-CSF and IL-6	Rhesus macaques exposed to 4 Gy ^{60}Co TBI; delivery 3-4 hr post-IR; hematopoietic recovery	FDA IND approval	Grace 2012, Stickney 2006, Whitnall 2005
ON01210 (Ex-RAD/Recilisib)	Radioprotector and mitigator	Chlorobenzylsulfone derivative	Tyrosine kinase inhibitor; attenuation of ATM/p53 signaling; upregulation of PI3K signaling	C3H/HeN mice exposed to 6 Gy TBI ^{60}Co; delivery 24 hr and 15 min pre-IR; mitigated neutropenia and bone marrow suppression; increased survival	FDA IND approval	Ghosh 2012, Singh 2015, Kang 2013
rhIL12 (HemaMax)	Radiomitigator	Recombinant cytokines	Cytokine; inflammatory regulator; stimulates IFN-γ production, macrophages and T-cells	Rhesus macaques exposed to 7 Gy TBI Co-60; delivery 1 day post-IR; increased survival	FDA IND approval	Basile 2012, Gluzman-Poltorak 2014
CBLB502 (Entolimid)	Radioprotector and mitigator	Flagellin derived protein	Toll-like receptor 5 agonist; stimulates NF-κB signaling; stimulates G-CSF; free radical scavenger	Rhesus macaques exposed to 6.5 Gy TBI Co-60; delivery 45 min pre-IR; increased survival	FDA IND approval and orphan drug status	Burdelya 2008, Singh 2015, Rosen 2015
PLacental eXpanded (PLX-R18)	Radiomitigator	Placental stromal cells with fetal offspring cells	Immunomodulator; secretes cytokines, chemokines and growth factors	C3H/HeN mice exposed to 7.7 Gy TBI 6–18 MeV LINAC; delivery 24 hr and 5 days post-IR; increased bone marrow hematopoietic cell proliferation	Research ongoing; plans to pursue FDA animal rule approval	Gaberman 2013
CLT-008	Bridging therapy	Myeloid progenitor cells	Stimulates myeloid, erythroid and dendritic cell development; provides hematopoietic support	CD2F1 mice exposed to 9 Gy TBI ^{60}Co; delivery 2hr or 2 day or 4 days or 7 days post-IR; increased survival	In clinical trials for patients with hematological malignancies	Singh 2012, 2015
BIO 300 (Genestein)	Radioprotector	Soy isoflavone, phytoestrogen	Antioxidant; free radical scavenger; protein tyrosine kinase inhibitor; cell cycle modulator	CD2F1 mice exposed to 9.25 Gy TBI ^{60}Co; delivery 24 hr pre-IR; increased survival; improved hematopoietic recovery	FDA IND approval	Ha 2013
CDX-301	Radioprotector and mitigator	Recombinant human protein form of the Fms-related tyrosine kinase 3 ligand (FLT3L), a hematopoietic cytokine	stimulates expansion and differentiation of hematopoietic progenitor and stem cells	C57BL/6 mice exposed to 7.76 TBI with ^{137}Cs source; delivery 24 hr pre-IR and 4 or 24 hr post-IR; increased survival	NHP studies underway at AFRRI	Thomas 2013

ALXN4100TPO	Radioprotector and mitigator	Thrombopoietin (TPO) receptor agonist	Activates thrombopoietin receptor; stimulates platelet production	CD2F1 mice exposed to 9 Gy TBI ^{60} Co; delivered 24hr pre-IR or 6 hr post-IR; abrogated thrombocytopenia and bone marrow atrophy	Research ongoing	Cary 2012, Satyamitra 2011
WR-638 (Cystaphos)	Radioprotector	Aminoethylphosphor-othioate	Antioxidant; free radical scavenger; DNA protector	Mice exposed to 7.5Gy TBI ^{60}Co; delivered 30 min pre-IR; antimutagenic	Carried in field pack by Russian army	Hall, Method for protection against genotoxic mutagenesis
Captopril and angiotensin converting enzyme (ACE) inhibitors	Radiomitigator	Anti-hypertensive drug	Thiol mediated free radical scavenger	C57BL/6 mice exposed to 6 or 7.5 Gy TBI ^{60}Co; delivery pre-IR and varying regimen post-IR; delivery pre-IR conferred no protection; post-IR treatment increased survival and abrogated thrombocytopenia	Research ongoing	Davis 2010
3,3'-Diindolylmethane (DIM)	Radioprotector and mitigator	Small molecule compound from the hydrolyzation of indole-3-carbinol (I3C)	Stimulates ATM signaling; DNA protector	Sprague–Dawley (SD) rats and C57BL/6 mice exposed to 13 Gy TBI 60Co; delivery post-IR 10min followed by 1x/day for 14 days; increased survival	In clinical trials for other indications	Fan 2013
Oltipraz	Radioprotector	Synthetic ditholethione derived from broccoli	Increased expression of microsomal epoxide hydrolase and glutathione S-transfer genes	Mice exposed to 8 Gy TBI gamma; delivery pre-IR; increased survival	In clinical trials for liver fat reduction and lung cancer prevention	Singh 2014
LY294002 or PX-867	Radiomitigator	Morpholine containing chemical compound	Phosphoinisitide-3 kinase (PI3K) inhibitor	C57BL/6NTac exposed to 9.25 Gy TBI with ^{137}Cs; delivery 10 min, 4 h, 24 h, or 48 h post-IR; extends survival; abrogated cell death	In clinical trial for neuroblastoma	Zellefrow 2012, Lazo 2013
Minocycline	Radioprotector and mitigator	2nd generation tetracycline derivative	Antibiotic; antioxidant; free radical scavenger	C57BL/6 mice exposed to 1-3Gy TBI ^{60}Co; delivery 10min pre-IR then 10 min post-IR and 1x/day for 3 days post-IR; Modulates production of cytokines	In clinical trials for neuroprotection during radiotherapy	Mehrotra 2012, Kim 2009, Tikka 2001
FGF-peptide	Radiomitigator	Synthetic binding domain peptide of FGF-2 with peptidase resistant dimer form	Maintains stem cell pool; promotes differentiated cells	NIH Swiss mice exposed to 6 Gy TBI with ^{137}Cs; delivery 48hr post-IR 1x/day for 5 days then 1x/day every other day for 10 days; increased the number of pro-B and pre-B cells	Research ongoing	Casey-Sawicki 2014

Fluoroquinolones	Radioprotector and mitigator	Broad-spectrum antibiotics that act against gram-positive and gram-negative bacteria	Antibiotic; antioxidant; free radical scavenger	C3Hf/Kam mice exposed to 8Gy TBI with ^{137}Cs; delivery 24 hr or 1 hr pre-IR or 24 hr post-IR then 5x/day; increased survival; enhanced hematopoiesis	In clinical trials for antimicrobial indications	Kim 2009, Shalit 1997
Octadecenyl Thiophosphate (OTP)	Radioprotector and mitigator	Small Molecule Mimic of Lysophosphatidic Acid	Receptor-mediated direct action; regulation of hematopoietic cytokine production	C57BL/6 mice exposed to 6.3 Gy TBI ^{137}Cs; delivery 12 hr pre-IR or 24, 48 and/or 72 hr post-IR; increased survival; enhanced hematopoiesis	Research ongoing	Deng 2015

Dietary Supplements:

Countermeasure	Class	Group	Mechanism	Testing	Status	References
Ascorbic Acid (Vitamin C)	Radioprotector and mitigator	Dietary supplement	Antioxidant; free radical scavenger	C57BL/6 mice exposed to 7 to 8 Gy TBI X-ray; delivery immediately pre-IR or post IR or 1, 6, 12, 24, 36 or 48 hr post-IR; increased survival	Regulated by FDA as a dietary supplement	Sato 2015
γ- Tocotrienol (GT3)	Radioprotectant	Small molecule; vitamin E isomer	DNA protector; antioxidant; stimulates G-CSF	CD2F1 mice exposed to 9.2 Gy TBI ^{60}Co; delivery 24 hr pre-IR; reduced DNA damage; reduced nitrosative stress; induced G-CSF	NHP studies underway at AFRRI	Kulkarni 2013, Singh 2014
δ – Tocotrienol (DT3)	Radioprotectant	Small molecule; vitamin E isomer	DNA protector; antioxidant; immunomodulator	CD2F1 mice exposed to 7–12.5 Gy TBI ^{60}Co; delivery 24 hr pre-IR; anti-apoptosis; induces cytokines increased survival	Research ongoing	Li 2015, Singh 2014
Mentha Piperita (Linn.) - peppermint	Radioprotector	Herb	antioxidant	Swiss albino mice exposed to TBI of 4,6,8 or 10Gy ^{60}Co; delivery 3 days pre-IR; inhibited radiation induced GSH depletion; decreased LPO; increased phosphatase	Herb; not regulated by FDA	Samarth 2003
Dragon's Blood and extracts	Radioprotector	Resin from the fruit of Daemonorops draco tree	anti-inflammatory; anti-apoptotic	BALB/c mice exposed to 4Gy TBI ^{60}Co; delivery 1x/day for 5 days pre-IR and 1x/day for 1, 3, 7 or 28 days post-IR; mitigated oxidative stress in the liver and spleen; enhance immunity; hemostasis	Herb; not regulated by FDA	Ran 2014, Xin 2012

α-Lipoic acid	Radioprotector	Organosulfur compound	lipophilic antioxidant	CD2F1 mice exposed to TBI of 9Gy ^{60}Co; delivery 30 min pre-IR; increased survival; dihydrolipoic acid had no radioprotective effect	Regulated by FDA as a dietary supplement	Ramakrishnan 1992

Radiation Countermeasures for Gastrointestinal Syndrome

Countermeasure	Class	Group	Mechanism	Testing	Status	References
ON01210 (Ex-RAD/Recilisib)	Radioprotector and mitigator	Chlorobenzylsulfone derivative	Tyrosine kinase inhibitor; attenuation of ATM/p53 signaling; upregulation of PI3K signaling	C3H/HeN mice exposed to 13 and 14 Gy TBI ^{60}Co; delivery 24 hr and 15 min pre-IR; preserved intestinal crypt cells	FDA IND approval	Ghosh 2012, Singh 2015, Kang 2013
Cerium oxide nanoparticles	Radioprotector	Oxide of the rare earth metal Cerium	Free radical scavenger; superoxide dismutase 2 regulator	Athymic nude mice exposed to 20Gy; delivery 4x pre-IR; protected GI epithelium by ROS scavenging and increasing production of SOD2	Research ongoing	Colon 2009, 2010, Baker 2013
TP508 (Chrysalin)	Radiomitigator	Rousalatide acetate regenerative peptide	stimulates expression of adherens junction protein E-cadherin; activates crypt cell proliferation; decreases apoptosis	Animals exposed to 9Gy TBI gamma radiation; delivery 24 post-IR; reduced GI toxicity; increased survival	Pursuing FDA approval under Animal Rule Guidance	Kantara 2015
Pectin	Radioprotector	Dietary supplement; highly-complex branched polysaccharide fiber; rich in galactoside residues; present in all plant cell walls	Inhibition of Notch signaling; anti-inflammatory	C57BL/6 mice exposed to 14 Gy TBI ^{137}Cs; delivery 1 week pre-IR and continued post-IR; prevents IR-induced deletion of potential reserve ISCs; facilitated crypt regeneration; increased survival	In clinical trials for intestinal support	Sureban 2015
OrbeShield/BDP	Radiomitigator	oral beclomethasone 17,21-dipropionate; corticosterioid	Induction of the Wnt-b-catenin pathway; Anti-inflammatory; vasoconstrictor	Canines exposed to 12Gy TBI; delivery 2 hr or 24 hr post-IR; increased survival; reduce epithelium damage	FDA IND for GI ARS; FDA Orphan Drug Designation for ARS	Soligenix
Anti-ceramide antibody (2A2)	Radioprotector	Inflammatory molecule	Transmits apoptotic signals; support recovery of crypt stem cell clonogens	C57BL/6 mice exposed to 15Gy TBI ^{137}Cs; delivery 15 min pre-IR; inhibits radiation-induced endothelial apoptosis and crypt lethality; increased survival	Research ongoing	Rotolo 2012

R-spondin1 (Rspo1)	Radioprotector	Protein	Increase stem cell population; inhibit radiation induced apoptosis in crypt; stimulation of Wnt-b-catenin signaling in RIGS	C57Bl/6 mice exposed to 10.4Gy TBI ^{137}Cs; delivery of recombinant adenovirus expressing human R-spondin1 using adenoviral gene transfer 1-3 days pre-IR; promoted intestinal stem cell regeneration; increased survival	Research ongoing	Bhanja 2009
ON01210 (Ex-RAD)	Radioprotector and mitigator	Chlorobenzylsulfone derivative	Tyrosine kinase inhibitor; attenuation of ATM/p53 signaling; upregulation of PI3K signaling	C3H/HeN mice exposed to 13 and 14 Gy TBI ^{60}Co; delivery 24 hr and 15 min pre-IR; protected mucosal structure and crypt cells	FDA IND approval	Ghosh 2012, Singh 2015
δ – Tocotrienol (DT3)	Radioprotector	Small molecule; vitamin E isomer	DNA protector; antioxidant; immunomodulator	CD2F1 mice exposed to 10-12 Gy TBI ^{60}Co; delivery 24 hr pre-IR; protected intestinal tissue; decreased apoptosis; inhibited gut bacterial translocation	In clinical trials for support in radiation therapy	Li 2013
N-Acetyl Cysteine (NAC)	Radioprotector and mitigator	Amino acid	Antioxidant	C57BL/6 mice abdomen exposed to 20 Gy X-ray Delivery 4hr pre-IR or 2hr post-IR and 1x/day for 6 days post-IR;increased survival	FDA approved to treat overdose of acetominophen	Jia 2010
α – tocopherol succinate (TS)	Radioprotector	Small molecule; vitamin E isomer	DNA protector; antioxidant; immunomodulator	CD2F1 mice exposed to 11 Gy TBI 60Co; delivery 24 hr pre-IR; protected intestinal tissue; improved structural integrity, inhibited apoptosis; enhanced cell	In clinical trials for support in radiation therapy	Singh 2013
SOM230 (Pasireotide)	Radioprotector and mitigator	Somatostatin analog	Preserves intestinal barrier function by decreased secretion of pancreatic enzymes	CD2F1 mice exposed to 8.5-11Gy TBI ^{137}Cs; delivery 24-72hr post-IR twice daily for 14 days; suppression of secretion of pancreatic enzymes; increased survival	Research ongoing with BARDA funding at UAMS	Fu 2011, Singh 2015
Octadecenyl Thiophosphate (OTP)	Radioprotector and mitigator	Small Molecule Mimic of Lysophosphatidic Acid	Anti-apoptotic agent	C57BL/6 mice exposed to 10.6 Gy TBI ^{137}Cs; delivery 2 hr pre-IR or 24hr post-IR; increased survival;restored glucose absorption and inhibited endotoxemia; significantly increased the number of regenerating crypts in the jejunum	Research ongoing	Deng 2015

Palifermin	Radioprotector	Recombinant N-terminal truncated form of keratinocyte growth factor (KGF)	Proliferation stimulation; anti-apoptotic	C57BL/6J mice exposed to 6 Gy TBI ^{60}Co; delivery 1x/day for 5 days pre-IR; improved distribution of tight junction proteins and epithelial barrier dysfunction	Phase I/II/II/IV clinical trials for oral mucositis in patients with head and neck cancer; stem cell transplant immune recovery	Singh 2014, Cai 2013

Radiation Countermeasures for Skin

Countermeasure	Class	Group	Mechanism	Testing	Status	References
PrC-210	Radioprotector	aminothiol	Antioxidant; free radical scavenger; DNA protector	Rats backs exposed to 17.3 or 41.7Gy ^{137}Cs; 4 topical applications delivered 2hr, 1hr, 30 min and 10 min pre-IR; 98% prevention of radiation dermatitis	Clinical trials for safety and efficacy for radiotherapy patients	Peebles 2012
FGF-peptide	Radiomitigator	Synthetic binding domain peptide of FGF-2 with peptidase resistant dimer form	Increases proliferation of keratinocytes; regulation of tight junction proteins	BALB/C mice exposed to 50Gy strontium; delivered topically and systemically daily for 16 days; accelerated wound healing	Research ongoing	Zhang 2011
Pravastatin	Radiomitigator	Statin	Anti-oxidant; anti-inflammatory	Balb/c mice exposed to 45 Gy TBI ^{60}Co; delivery in food daily post-IR for 28 days; Modulated cytokines; limits downregulation of endothelial nitric oxide synthase	FDA approved for treatment of high cholesterol	Holler 2009
Plerixafor	Radiomitigator	bicyclam compound	CXCR-4 antagonist;bone marrow stem cell mobilizer	C57BL/6 mice exposed to 25-30 Gy X-ray; delivery of 2 doses with 2 days between started either on day 0, 4, 7, 15 or 24 post-IR; improves both acute and late skin response to radiation exposure	FDA approval for immobilizing stem cells in non-hodgkin lymphoma and multiple myeloma	Kim 2012
Curcumin	Radioprotector and mitigator	Diarylheptanoid; phenol	Anti-inflammatory; regulator of cytokines; antioxidant	C3H/HeN mice exposed to 50Gy; delivery 5 days pre-IR or 5 days post-IR or 5 days pre-IR and 5 days post-IR; reduced acute and chronic skin toxicity	In clinical trials for radiation dermatitis	Okunieff 2006, Ryan 2013

Radiation Countermeasures for Lung, Esophagus, Oral, Heart						
Countermeasure	**Class**	**Group**	**Mechanism**	**Testing**	**Status**	**References**
Manganese Superoxide Dismutase (MnSOD)	Radimitigator	Protein	Anti-apoptotic; metabolizes reactive oxygen species	9.5 Gy TBI; MnSOD combined with antioxidant diet extends life after ARS recovery	In clinical trial for protection of radiation induced esophagitis	Borelli 2009
Rapamycin	Radioprotector	Small molecule	MTOR inhibitor; blocks radiation induced cellular senescence	C3H mice exposed to 30 Gy fractionation (6 Gy weekly); delivery 1x/week; protects from the loss of proliferative basal epithelial stem cells; reduced DNA damage; did not confer protection when delivered with single dose of 15 Gy	In clinical trials for head and neck cancer; NSCLC	Iglesias-Bartolome 2012, Rosen 2015
Transforming growth Factor β3 (TGFβ3)	Radiomitigator	Protein	Attenuates radiation induced pulmonary function	Mice exposed to a single thoracic radiation of 20Gy; delivery weekly; decelerated progress of radiation induced fibrosis; slowed recruitment of fibrocytes; Th1 response suppressed	Research ongoing	Xu 2014, Rosen 2015
AEOL 10150	Radioprotector and mitigator	Metalloporphyrin	Antioxidant; free radical scavenger	Rhesus macaques exposed to 11.5 Gy of whole thorax lung irradiation; delivery 24 hr post-IR daily for 4 weeks; reduced incidence of radiation induced lung injury	FDA Orphan Drug Designation for ARS	Garofalo 2014
Palifermin (Kepivance)	Radioprotector	Recombinant N-terminal truncated form of keratinocyte growth factor (KGF)	Proliferation stimulation; anti-apoptotic	C57BL/6J mice exposed to 6 Gy TBI ^{60}Co; delivery 1x/day for 5 days pre-IR; recovery of mucosa	Phase I/II/II/IV clinical trials for oral mucositis in patients with head and neck cancer; stem cell transplant immune recovery	Singh 2014, Cai 2013
Cerium oxide nanoparticles	Radioprotector	Oxide of the rare earth metal Cerium	Free radical scavenger; superoxide dismutase 2 regulator	Athymic nude mice exposed to 30Gy fractionation (5 Gy weekly); delivery 2x/week; no visible pneumonitis	Research ongoing	Colon 2009, 2010, Baker 2013

Melatonin	Radioprotector	hormone	Free radical scavenging; singlet oxygen quenching	Wistar rats exposed to 18Gy 2.5x2.5cm area of ^{60}Co; delivery 15 min pre-IR; vasculitis prevented; decreased fibrosis and myocyte necrosis; cardioprotective Wistar rats exposed to 18Gy 2.5x2.5cm area of 60Co; delivery 15 min pre-IR; lung injury reduced; fibrosis still present	Regulated by FDA as a dietary supplement	Gurses 2014, Serin 2007, Tahamtan 2015

Radiation Countermeasures Tested in Space Radiation Simulated Environment

Countermeasure	Class	Group	Mechanism	Testing	Status	References
Selenomethionine (SeM)	Radioprotector	Dietary antioxidant	Maintains activities of the antioxidant enzymes glutathione peroxidase and thioredoxin reductase; regulate expression of genes involved in the repair of radiation-induced DNA damage	Sprague-Dawley Rats exposed to 1 Gy ^{56}Fe ions; delivery of SeM in diet 3 days pre-IR; decreased total antioxidant status	FDA approval as dietary supplement	Kennedy 2003
Eusatron and Ondansetron (Zofran)	Anti-Emetic	5-hydroxytryptamine (5-HT3)	serotonin subtype-three receptor antagonist	Ferrets exposed to 2Gy TBI 2-Gy doses of either ^{60}Co gamma or neutron:gamma, mixed-field irradiation; delivery post-IR; mitigated emesis	FDA approved to prevent nausea and vomiting; currently in ISS medical kit	King 1999
Manganese Superoxide Dismutase (MnSOD)	Radiomitigator	Protein	Anti-apoptotic; metabolizes reactive oxygen species	CBAxC57Bl6 F1 hybrid SPF mice exposed to 4Gy 171MeV protons;delivery 6x/day; accelerated recovery of thymus and spleen mass and of the number of leukocytes in mice peripheral blood	In clinical trial for protection of radiation induced esophagitis	Ambesi-Impiombato 2014
Neupogen	Radiomitigator	Recombinant growth factor	Granulocyte Colony Stimulating Factor (G-CSF)	ICR mice exposed to 0.5, 1 or 2 Gy ^{137}Cs or SPE-like proton; delivery 1 day pre-IR, immediately post-IR or 1 day post-IR; increased neutrophil counts	FDA approval under Animal Rule for ARS	Romero-Weaver 2013

Neulasta (pegylated form of Neupgen)	Radiomitigator	Pegylated growth factor	Granulocyte Colony Stimulating Factor (G-CSF)	Yucatan mini pigs exposed to 2 Gy TBI SPE-like protons; temporarily alleviates proton radiation-induced WBC loss, but has no effect on altered hemostatic responses	NHP studies conducted for FDA approval to treat ARS under Animal Rule	Sanzari 2015
Cocktail: SeM, α-lipoic acid, NAC, sodium ascorbate and Vitamin E succinate	Radioprotector	Dietary antioxidant cocktail	Anti-apoptotic; reactive oxygen species scavengers	ICR mice exposed to 1 or 7Gy TBI ^{137}Cs; fed cocktail diet for 7 days pre-IR; second group began cocktail diet 2 hr post-IR; no attenuation of lymphopenia; attenuated the radiation-induced inflammatory response and hematopoietic cell death ICR mice exposed to 1Gy proton; fed cocktail diet for 7 days pre-IR; second group began cocktail diet 2 hr post-IR; improved recovery of peripheral leukocytes and platelets	Research ongoing	Kennedy 2006, Wambi 2008, 2009, Sanzari 2011
Fructose	Radioprotector and mitigator	monosaccharide	Immune modulation; oxidative protection	ICR mice exposed to 2 Gy TBI ^{137}Cs gamma or SPE-like proton; delivery of fructose daily for 7 days pre-IR continuing post-IR or daily for 7 days pre-IR; increase the numbers of lymphocytes	No known studies ongoing	Romero-Weaver 2014
Enrofloxacin	Radiomitigator	broad-spectrum orally available antibiotic	Anti-microbial	C3H/HeNCr MTV- mice exposed to 2Gy ^{137} Cs or SPE-like protons; delivery 5 days post-IR 2x/day until the end; enhanced bacterial clearance and significantly decreased morbidity and mortality	No known studies ongoing	Li 2015
Mometasone cream (Elecon)	Radiomitigator	Corticosteroid	Anti-inflammatory; antipruritic; vasoconstrictive	Yucatan mini pigs exposed to 5 or 10 Gy TBI proton; delivered topically 1x/day and covered with Tegaderm post-IR for 14 days; mitigated skin toxicity; decreased melanosomes, necrotic keratinocytes and melanin deposition	FDA approved for psoriasis and dermatitis	Kennedy 2014

Benefix	Radiomitigator	Recombinant protein factor IX	Replaces the missing clotting factor IX that is needed for effective hemostasis	De-scented ferrets exposed to 1Gy TBI SPE-like protons;delivery 30 min pre-IR; improved clotting values in the irradiated ferrets	FDA approval for hemophilia B	Krigsfeld 2013
Bowman-Birk Inhibitors (BBI)	Radioprotector and mitigator	Protease inhibitor	Antioxidant	CBA/JCR HSD exposed to 0.5Gy ^{56}Fe ions or 3Gy protons; delivered in food 3 days pre-IR then daily post-IR; reduced yields of neoplastic lesions; no impact on survival	FDA IND	Kennedy 2006, 2008
Blueberry or Strawberry Extracts	Radioprotector	Antioxidant	Free radical scavenging, polyphenols	Sprague–Dawley rats exposed to 1.5 Gy of 1 GeV/n ^{56}Fe particles; delivery 2% blueberry or strawberry extracts 2 months pre-IR; 2% strawberry extract can prevent the disruption of responding on an ascending fixed-ratio operant task	Research ongoing	Rabin 2005
Androstenediol (5-AED)	Radioprotector and mitigator	Steroid	Nuclear Factor-κβ; increases G-CSF and IL-6	C57BL/6J mice exposed to 3Gy ^{56}Fe; delivery 30 min post-IR; restored hematopoiesis	FDA IND approval	Loria 2011
Dragon's Blood and extracts	Radioprotector	Resin from the fruit of Daemonorops draco tree	anti-inflammatory; anti-apoptotic	Wistar rats exposed to 2.5Gy whole head $^{12}C^{6+}$ heavy ions; delivery 1x/day for 5 days pre-IR then 1x/day until endpoint; decreased malondialdehyde and hydrogen peroxide levels; increased SOD activity and glutathione levels; decreased inflammatory cytokines	Herb; not regulated by FDA	Xin 2012
Vitamin A acetate (retinol acetate)	Radioprotector	Vitamin	Anti-inflammatory; MMP inhibitor	Sprague-Dawley rats dorsal skin exposed to 3Gy ^{56}Fe ions; delivery 1 week in food pre-IR continuing post-IR until endpoint; decreased expression of immune- and stress-response genes	FDA approval as dietary supplement	Zhang 2006
Fish oil and pectin	Radioprotector	Dietary supplements	Inhibition of Notch signaling; anti-inflammatory	Sprague–Dawley rats exposed to 1 Gy of 1 GeV/n ^{56}Fe particles; delivery of fish oil and pectin in diet 3 weeks pre-IR; suppressed antiapoptotic PPARδ levels	FDA approval as dietary supplements	Vanamala 2008

α-Lipoic acid	Radioprotector and mitigator	Organosulfur compound	lipophilic antioxidant	hippocampal precursor cells exposed to 1 Gy of 1 GeV/n ^{56}Fe particles; delivery 1 hr pre-IR or 2hr post-IR; reduced reactive oxygen species	Regulated by FDA as a dietary supplement	Limoli 2007
Amifostine (Ethyol) or WR-1065, WR-2721, WR-151,327	Radioprotector	Aminothiol	Antioxidant; free radical scavenger; DNA protector	CHO. S31WT clone, MCF10A, and SPD8 Chinese hamster cells exposed to 2 Gy of X rays; delivery of WR-1065 with 30 min or 24 hr incubation of CM; prevented hyper-recombination and mutagenesis	FDA approval for renal toxicity and xerostemia in patients being treated for cancer	Dziegielewski 2010

VII. Gaps

Current research is focused on closing the following knowledge gaps:

Acute–1: Determine the dose response for acute effects induced by SPE-like radiation, including synergistic effects (focusing on effects that are evident at space-relevant doses) arising from other spaceflight factors (microgravity, stress, immune status, bone loss, etc.) that modify and/or enhance the biological response. (Note: Acute-1 and Acute-3 were combined into Acute-1).

Acute–2: What quantitative procedures or theoretical models are needed to extrapolate molecular, cellular, or animal results to predict acute radiation risks in astronauts? How can human epidemiology data best support these procedures or models?

Acute–4: What are the probabilities of hereditary, fertility, and sterility effects from space radiation? (On hold pending evidence of risk at space relevant exposures)

Acute–5: What are the optimal SPE alert and dosimetry technologies? (**Closed**. Technology maturation transferred to Advanced Exploration Systems)

Acute–6: What are the most effective shielding approaches to mitigate acute radiation risks, how do we know, and implement? (**Closed**. Transferred to Operations)

Acute–7: What are the most effective biomedical or dietary countermeasures to mitigate acute radiation risks?

Acute–8: How can probabilistic risk assessment be applied to SPE risk evaluations for EVA, and combined EVA+IVA exposures?

The SRPE overlaps with several of the gaps within other HRP Elements as outlined in the HRP Integrated Research Plan (IRP). SRPE works with the other HRP Elements to integrate gaps as necessary in accordance with the IRP.

VIII. Conclusion

The biological effects of space radiation, including ARS, are a significant concern for manned spaceflight. The primary data that are currently available are derived from analyses of medical patients and persons accidentally exposed to high doses of radiation. High doses of radiation can induce profound radiation sickness and death. Lower doses of radiation induce symptoms that are much milder physiologically but that pose operational risks that may be equally serious. Both scenarios have the potential to seriously affect crew health and/or prevent the completion of mission objectives. NASA has established short-term dose limits to prevent clinically significant deterministic health effects, including performance degradation in flight. Radiation protection must be provided in the form of shielding and operational dosimetry and monitoring, as well as biological countermeasures (if an unavoidable exposures is encountered), when traveling outside of the protective magnetosphere of Earth. Predictive models support the evaluation of crew

risks, operational requirements and decisions, and the efficient design of vehicle shelters to minimize exposures.

As future NASA missions once again extend beyond LEO and now for longer durations, radiobiology research is focused on validating the current PELs, as there is reasonable concern that a compromised immune system due to high skin doses from a SPE or due to synergistic space flight factors (e.g., microgravity) may lead to increased risk to the BFO. Research data specific to the space flight environment are being compiled to quantify the magnitude of this increased risk and to develop appropriate predictive models and protection strategies. In addition, clinically relevant biological countermeasures or those developed for counterterrorism are being identified and validated for spaceflight-relevant exposures, which are characterized by different radiation qualities and dose rates than those associated with terrestrial applications.

IX. References

Adelstein SJ, Dealy JB (1965) Hematologic responses to human whole-body irradiation. Am. J Roentgenol Rad Therapy Nuc Med 93:927–934

Adriani O, Barbarino GC, Bazilevskaya GA et al (2015) PAMELA's Measurements of magnetospheric effects on high-energy solar particles. Astrophys J Lett 801:L3

Ainsworth J (1986) Early and late mammalian responses to heavy charged particles. Adv Space Res 6:153-165

Alexander GA, Swartz HM, Amundson SA et al (2007) BiodosEPR-2006 Meeting:acute dosimetry consensus committee recommendations on biodosimetry applications in events involving terrorist uses of radioactive materials and radiation accidents. Radiat Meas 42:972-996

Ambesi-Impiombato FS, Belov O, Bulinina T, Ivanov A, Mancini A, Borrelli A, Krasavin EA (2014) Recombinant human manganese superoxide dismutase (rMnSOD): a positive effect on the immunohematological state of mice irradiated with protons. 40th COSPAR Scientific Assembly. Aug 2014, in Moscow, Russia, Abstract F2.2-28-14

Amgen (2015) Highlights of prescribinginformation. http://pi.amgen.com/united_states/neupogen/neupogen_pi_hcp_english.pdf. Accessed 1 June 2015.

Andrews PLR, Morrow GR, Hickok JT et al (2004) Mechanisms and models of fatigue associated with cancer and its treatment: Evidence of pre-clinical and clinical studies. In: Armes J, Krishnasamy M, Higginson I (eds) Fatigue in Cancer, Oxford University Press, Oxford, pp 51–87

Anno GH, Wilson DB, Baum SJ (1985) Severity levels and symptom complexes for acute radiation sickness: description and quantification. Alexandria, VA: Defense Nuclear Agency, DNA-TR-86-94

Anno GH, Baum SJ, Withers HR, Young RW (1989) Symptomatology of acute radiation effects in humans after doses of 0.5-30 Gy. Health Phys 56:821–838

Anno GH, McClellan GE, Dore MA, Baum SJ (1991) Biological effects of protracted exposure to ionizing radiation: review, analysis, and model development. Alexandria, VA: Defense Nuclear Agency, DNA-TR-90-157

Anno GH, McClellan GE, Dore MA (1996) Protracted radiation-induced performance decrement, Vol. 1 – Model development. Defense Nuclear Agency Report DNA-TR-95-117-V1. Defense Nuclear Agency, Alexandria, Va

Aran A, Sanahuga B, Lario D (2005) Fluxes and fluences of SEP events derived from SOLPENCO. Annales Geophysicae 23:3047-3053

Archambeau JO, Bennett GW, Abata JJ and Brenneis HJ (1979) Response of swine skin to acute single exposures of X rays: quantification of the epidermal cell changes. Radiat Res 79: 298-337

Atwell W, Beever ER, Hardy AC et al (1987) Space radiation shielding analysis and dosimetry for the space shuttle program. AIP Conf Proc 186:289-296

Babior BM, Golde DW (2001) Production, distribution, and fate of neutrophils. In: Beutler E, Coller BS, Lichtman MA, Kipps TJ, Seligsohn U (eds) Williams hematology, McGraw-Hill, New York, pp 753–759

Badhwar GD, Atwell W, Reitz G, Beaujean R, Heinrich W (2002) Radiation measurements on the Mir Orbital Station. Radiat Meas 35:393-422

Baker C (2013) Harnessing cerium oxide nanoparticles to protect normal tissue from radiation damage. Transl Cancer Res 2(4):343-358

Band D, Matteson J, Ford L et al (1993) BATSE observations of gamma-ray burst spectra. I. Spectral diversity. Astrophys J 413:281-292

Baum SJ, Young RW, Anno GH, Withers HR (1984) Symptomatology of acute radiation effects in human after exposure to doses of 75 to 4500 rads (cGy) free-in-air. In: Nuclear Weapons Effect Research at PSR-1983, Vol 10. Pacific-Sierra Research Corporation Report, National Technical Information Service, Springfield, Va, Defense Nuclear Agency DNA-TR-85-50

Basile L, Ellefson D, Gluzman-Poltorak Z et al (2012) HemaMax™ a Recombinant Human Interleukin-12, is a Potent Mitigator of Acute Radiation Injury in Mice and Non-Human Primates. PLOS One 7(2):e30434

BEIR VII (2006) Health risks from exposure to low levels of ionizing radiation: BEIR VII – Phase 2 committee to assess health risks from exposure to low levels of ionizing radiation. National Research Council. National Academies Press, Washington, DC

Belka C, Marini P, Budach K et al (1998) Radiation induced apoptosis in human lymphocytes and lymphoma cells critically relies on the up-regulation of CD95/Fas/APO-1 ligand. Radiat Res 149:588–595

Bhanja P, Saha S, Kabarriti R, Liu L, Roy-Chowdhury N, Roy-Chowdhury J, Sellers RS, Alfieri AA, Guha C (2009) Protective Role of R-spondin1, an Intestinal Stem Cell Growth Factor, against Radiation-Induced Gastrointestinal Syndrome in Mice. PLoS ONE 4(11):e8014

Billings MP, Yucker WR (1973) The computerized Anatomical Man (CAM) Model. NASA CR-134043, Washington, DC

Blanpain C and Fuchs E (2009) Epidermal homeostasis: a balancing act of stem cells in the skin. Nat Rev Mol Cell Biol 10: 207-217

Blakely J (1968) The case of radiation casualties. Charles C. Thomas Company, Springfield, Ill.

Blakely WF, Salter CA, Prasanna PGS (2005) Early-response biological dosimetry: recommended countermeasure enhancements for mass-casualty radiological incidents and terrorism. Health Phys 89:494-504

Bogo V, Jacobs A, Weiss, J (1985) Behavioral toxicity and efficacy of WR-2721 as a radioprotectant. Radiat Res 104:182-190

Bond VP, Fliedner TM, Archambeau JO (1965) Mammalian radiation lethality. Academic Press, New York

Borelli A, Schiattarella A, Mancini R et al (2009) A recombinant MnSOD is radioprotective for normal cells and radiosensitizing for tumor cells. Free Radic Biol Med 46(1):110-116

Borison HL (1989) Area postrema: chemoreceptor circumventricular organ of the medulla oblongata. Prog Neurobiol 32: 351-90

Bourgier C, Levy A, Vozenin MC, Deutsch E (2012) Pharmacological strategies to spare normal tissues from radiation damage: useless or overlooked therapeutics? Cancer Metastasis Rev 31:699-712

Bouville A, Chumak VV, Inskip PD, Kryuchkov V, Luckyanov, N (2006) The Chernobyl accident: estimation of radiation doses received by the Baltic and Ukrainian cleanup workers. Radiat Res 166(1 Pt 2):158–167

Bower JE, Ganz PA, Aziz N et al (2002) Fatigue and proinflammatory cytokine activity in breast cancer survivors. Psychosom Med 64:604–611

Brown W (1953) Symptomatic disturbance after single-therapeutic dose of x-rays. Br Med J 1:802–80

Burdelya LG, Krivokrysenko VI, Tallant TC et al (2008) An agonist of toll-like receptor 5 has radioprotective activity in mouse and primate models. Science 320(5873):226-30

Cai Y, Wang W, Liang H, Sun L, Teitelbaum DH, Yang H (2013) Keratinocyte growth factor pretreatment prevents radiation-induced intestinal damage in a mouse model. Scand J Gastroenterol 48(4):419-426

Cary L, Ngudiankama B, Salber R, Ledney D, Whitnall M (2012) Efficacy of radiation countermeasures depends on radiation quality. Radiat Res 177:663-675

Casey-Sawicki K, Zhang M, Kim S et al (2014) A basic fibroblast growth factor analog for protection and mitigation against acute radiation syndromes. Health Phys 106(6):704-712

Cattanach BM, Burtenshaw MD, Rasberry C, Evans EP (1993) Large deletions and other gross forms of chromosome imbalance compatible with viability and fertility in the mouse. Nat Genet 3(1):56-61

Centola GM, Keller JW, Henzler M, Rubin P (1994) Effect of low-dose testicular irradiation on sperm count and fertility in patients with testicular seminoma. J Androl15(6):608-613

Colon J, Herrera L, Smith J, Patil S, Komanski C, Kupelian P, Seal S, Jenkins DW, Baker CH (2009) Protection from radiation-induced pneumonitis using cerium oxide nanoparticles. Nanomedicine 5(2):225-231

Colon J, Hsieh N, Ferguson A, Kupelian P, Seal S, Jenkins DW, Baker CH (2010) Cerium oxide nanoparticles protect gastrointestinal epithelium from radiation-induced damage by reduction of reactive oxygen species and upregulation of superoxide dismutase 2. Nanomedicine 6(5):698-705

Conklin JJ, Walker RI (1987) Diagnosis, triage and treatment of casualties. In: Conard RA, Walker RI (eds) Military radiobiology, Academic Press, Orlando FL, pp 231–240

Copp RR, Peebles DD, Soref CM, Fahl WE (2013) Radioprotective efficacy and toxicity of a new family of aminothiol analogs. Int J Radiat Biol 89(7):485–492

Cucinotta FA, Townsend LW, Wilson JW, Golightly MJ, Weyland M (1994) Analysis of Radiation Risk from Alpha Particle Component of Solar Particle Events. Adv Space Res 10:661–670

Cucinotta FA (1999) Issues in Risk Assessment from Solar Particle Events. Radiat Meas 30:261–268.

Cucinotta FA, Kim MY, Ren L (2006) Evaluating shielding effectiveness for reducing space radiation cancer risks. Radiat Meas 41:1173–1185

Cucinotta FA, Durante M (2006) Cancer risk from exposure to galactic cosmic rays: implications for space exploration by human beings. The Lancet Oncol 7:431– 435

Cucinotta FA, Hu S, Schwadron NA, Kozarev K, Townsend LW, Kim MY (2010) Space radiation risk limits and Earth-Moon-Mars environmental models. Space Weather 8:S00E09

Curt GA (2000) The impact of fatigue on patients with cancer: overview of FATIGUE 1 and 2. Oncologist 5(Suppl 2):9-12

Curtis SB (1986) Lethal and potentially lethal lesions induced by radiation—a unified repair model. Radiat Res 106:252–270

Dainiak N (2002) Hematologic consequences of exposure to ionizing radiation. Exp Hemat 30:513-528

Dainiak N, Gent RN, Carr Z et al (2011) Literature review and global consensus on management of acute radiation syndrome affecting nonhematopoietic organ systems. Disaster Med Public Health Prep 5(3):183-201

Damewood MD, Grochow LB (1986) Prospects for fertility after chemotherapy or radiation for neoplastic disease. Fertil Steril 45(4):443-459

Davis TA, Landauer MR, Mog SR, Barshishat-Kupper M, Zins SR, Amare MF, Day RM (2010) Timing of captopril administration determines radiation protection or radiation sensitization in a murine model of total body irradiation. Exp Hematol 38(4):270-281

Deng W, Kimura Y, Gududuru V et al (2015) Mitigation of the hematopoietic and gastrointestinal acute radiation syndrome by octadecenyl thiophosphate, a small molecule mimic of lysophosphatidic acid. Radiat Res 183(4):465-475

Dingli D, Traulsen A, Pacheco JM (2007) Compartmental architecture and dynamics of hematopoiesis. PLoS ONE 2:e345

Dubrova YE, Nesterov VN, Krouchinsky NG, Ostapenko VA, Neumann R, Neil DL, Jeffreys AJ. (1996) Human minisatellite mutation rate after the Chernobyl accident. Nature 380(6576):683-686.

Dubrova YE, Grant G, Chumak AA, Stezhka VA, Karakasian AN (2002) Elevated minisatellite mutation rate in the post-chernobyl families from ukraine. Am J Hum Genet (4):801-809

Dziegielewski J, Goetz W, Murley JS, Grdina DJ, Morgan WF, Baulch JE (2010) Amifostine metabolite WR-1065 disrupts homologous recombination in mammalian cells. Radiat Res 173(2):175-183

Evans JS, Moeller DW, Cooper DW (1985) Health Effects Model for Nuclear Power Plant Accident Consequences Analysis. NUREG/CR-4214 SAND857185, National Technical Information Service, Springfield, Va

Fan S, Meng Q, Xu J et al (2013) DIM (3,3′-diindolylmethane) confers protection against ionizing radiation by a unique mechanism. Proc Natl Acad Sci USA 110(46):18650–18655

Farese A, Brown C, Smith C, Gibbs A, Katz B, Johnson C, Prado K and MacVittie T (2013) The ability of filgrastim to mitigate mortality following LD50/60 total-body irradiation is administration time-dependent. Health Phys 106(1):39-46

Farese AM, Brown CR, Smith CP, Gibbs AM, Katz BP, Johnson CS, Prado KL, MacVittie TJ (2014) The ability of filgrastim to mitigate mortality following LD50/60 total-body irradiation is administration time-dependent. Health Phys 106(1):39-47

FDA (2015) FDA Approves Radiation Medical Countermeasure http://www.fda.gov/EmergencyPreparedness/Counterterrorism/MedicalCountermeasures/AboutMCMi/ucm443245.htm. Accessed 1 June 2015

Feyer, PC, Maranzano, E, Molassiotis, A, Clark-Snow, RA, Roila, F, Warr, D, Olver, I (2005) Radiotherapy-induced nausea and vomiting (RINV): antiemetic guidelines. Support Care Cancer 13:122-128

Feyer P, Jahn F, Jordan K (2014) Radiation induced nausea and vomiting. Eur J Pharmacol 722:165-171

Feynman J, Ruzmaikin A, Berdichevsky V (2002) The JPL proton fluence model: an update. Journal of Atmospheric and Solar-Terrestrial Physics 64:1679-1686

Fliedner TM, Tibken B, Hofer EP, Paul W (1996) Stem cell responses after radiation exposure: a key to the evaluation and prediction of its effects. Health Phys 70:787–797

Fliedner TM, Friesecke I, Beyrer K (2001) Medical Management of Radiation Accidents–Manual on the Acute Radiation Syndrome. British Institute of Radiology, London

Fliedner TM, Graessle D, Paulsen C, Reimers K (2002) Structure and function of bone marrow hemopoiesis: mechanisms of response to ionizing radiation exposure. Cancer Biother Radiopharm 17:405-426

Fliedner TM, Graessle D, Meineke V, Dorr H (2007) Pathophysiological principles underlying the blood cell concentration responses used to assess the severity of effect after accidental whole-body radiation exposure: an essential basis for an evidence-based clinical triage. Exp Hematol 35(Suppl 1):8-16

Freier PS, Webber WR (1963) Exponential rigidity spectrums for solar-flare cosmic rays. J Geophys Res 68(6):1605-1629

Fry DJ, Zapp N, Biesecker D, Leka KD, Barnes G, De Koning, CA (2010), Proceedings of the First All-Clear Forecasting Workshop, NASA JSC Houston, TX

Fu Q, Berbée M, Wang W, Boerma M, Wang J, Schmid HA, Hauer-Jensen M (2011) Preclinical evaluation of Som230 as a radiation mitigator in a mouse model: postexposure time window and mechanisms of action. Radiat Res 175(6):728-735

Fuchs E, Horsley V (2008) More than one way to skin. Genes Dev 22:976-985

Furusawa Y, Fukutsu K, Aoki M, Itsukaichi H, Eguchi-Kasai K, Ohara H, Yatagai F, Kanai T, Ando K (2000) Inactivation of aerobic and hypoxic cells from three different cell lines by accelerated He, C and Ne ion beams. Radiat Res 154:485–496

Gaberman E, Pinzur L, Levdansky L, Tsirlin M, Netzer N, Aberman Z, Gorodetsky R (2013) Mitigation of lethal radiation syndrome in mice by intramuscular injection of 3D cultured adherent human placental stromal cells. PLOS One 8(6):e66549

Gangloff H (1964) Hippocampal spike activity following low doses of irradiation. In: Haley TJ, Snider RS (eds) Response of the nervous system to ionizing radiation; 2nd International Symposium, Los Angeles. Little Brown, Boston, MA, pp 221–242

Garofalo MC, Ward AA, Farese AM, Bennett A, Taylor-Howell C, Cui W, Gibbs A, Prado KL, MacVittie TJ (2014) A pilot study in rhesus macaques to assess the treatment efficacy of a small molecular weight catalytic metalloporphyrin antioxidant (AEOL 10150) in mitigating radiation-induced lung damage. Health Phys 106(1):73-83

Ghosh SP, Kulkarni S, Perkins MW, Hieber K, Pessu RL, Gambles K et al (2012) Amelioration of radiation-induced hematopoietic and gastrointestinal damage by Ex-RAD® in mice. Jo of Radiat Res 53:526-36

Gilberti MV (1980) The 1967 radiation accident near Pittsburgh Pennsylvania, and a follow-up report. In: Hubner EF, Fry SA (eds) The medical basis for radiation accident preparedness. Elservier, North Holland, NY, pp 131–40

Gluzman-Poltorak Z, Vainstein V, Basile LA (2014) Recombinant interleukin-12, but not granulocyte-colony stimulating factor, improves survival in lethally irradiated nonhuman primates in the absence of supportive care: evidence for the development of a frontline radiation medical countermeasure. Am J Hematol 89(9):868-73

Goans, RE, Flynn, DF (2012) Acute Radiation Syndrome in Humans in Medical Consequences of Radiological and Nuclear Weapons edited by Mickelson, AB. Office of The Surgeon General, United States Army, Falls Church, Virginia. Borden Institute, Fort Detrick, Maryland, pp 17-38

Gong EJ, Shin IS, Son TG, Yang K, Heo K, Kim JS (2014) Low-dose-rate radiation exposure leads to testicular damage with decreases in DNMT1 and HDAC1 in the murine testis. J Radiat Res 55(1):54-60

Goswami JN, McGuire RE, Reedy RC, Lal D, Jha R (1988), Solar flare protons and alpha particles during the last three solar cycles. J Geophys Res 93(A7):7195–7205

Gowans JL (1959) The recirculation of lymphocytes from blood to lymph in the rat. J Physiol 46:54–69

Grace M, Singh, V, Rhee J, Jackson W, Kao TC, Whitnall M (2012) 5-AED enhances survival of irradiated mice in a G-CSF-dependent manner, stimulates innate immune cell function, reduces radiation-induced DNA damage and induces genes that modulate cell cycle progression and apoptosis. J Radiat Res 53:840-853

Grdina DJ, Murley JS, Miller RC, Mauceri HJ, Sutton HG, Thirman MJ, Li JJ, Woloschak GE, Weichselbaum RR (2013) A manganese superoxide dismutase (SOD2)-mediated adaptive response. Radiat Res 179(2):115-124

Gridley DS, Freeman TL, Makinde AY et al (2011) Comparison of proton and electron radiation effects on biological responses in liver, spleen and blood. Int J Radiat Biol 87(12):1173-1181

Gupta S (2013) BRIEFING PACKAGE FDA ADVISORY COMMITTEE MEETING 03 May 2013: TUDY DRUG: Leukine® (sargramostim)

Gürses I, Özeren M, Serin M, Yücel N, Erkal HŞ (2014) Histopathological evaluation of melatonin as a protective agent in heart injury induced by radiation in a rat model. Pathol Res Pract 210(12):863-871

Guskova AK, Baranov AE, Gusev IA (2001) Acute radiation sickness: underlying principles and assessment. In: Gusev IA, Guskova AK, Mettler FA Jr (eds) Medical management of radiation accidents, CRC Press, Boca Raton, Fl, pp 33-51

Ha C, Li XH, Fu D, Xiao M, Landauer M (2013) Genistein nanoparticles protect mouse hematopoietic system and prevent proinflammatory factors after gamma irradiation. Radiat Res 180:316-325

Hall EJ, Giaccia AJ (2006) Radiobiology for the Radiologist. Lippincott Williams & Wilkins, Philadelphia, PA

Hankey KG, Farese AM, Blaauw EC, Gibbs AM, Smith CP, Katz BP, Tong Y, Prado KL, MacVittie TJ (2015) Pegfilgrastim Improves Survival of Lethally Irradiated Nonhuman Primates. Radiat Res 183(6):643-655

Haskin FE, Harper FT, Gooseens LH, Kraan BCP, Grupa JB, Randall J (1997) Probabilistic accident consequence uncertainty analysis: Early health effects uncertainty assessment. Main Report. NUREG/CR-6545, EUR 15855 Vol. 1, US Nuclear Regulatory Commission, Washington, DC

Hirama T, Tanosaki S, Kanatsu S et al (2003) Initial medical management of patients severely irradiated in the Tokai-mura criticality accident. Br J Radiol 76(904):246–253

Holler V, Buard V, Gaugler MH, Guipaud O, Baudelin C, Sache A et al (2009) Pravastatin limits radiation-induced vascular dysfunction in the skin. J Invest Dermatol 129:1280-1291

Horn CC, Ciucci M, Chaudhury A (2007) Brain Fos expression during 48 h after cisplatin treatment: neural pathways for acute and delayed visceral sickness. Auton Neurosci 132:44-51

Hornby PJ (2001) Central neurocircuitry associated with emesis. Am J Med 111(Suppl 8A):106S-112S

Hu S, Kim MY, McClellan GE, Cucinotta FA (2009) Modeling the acute health effects of astronauts from exposures to large solar particle events. Health Phys 96(4):465–476

Hu S, Cucinotta FA (2011a). A cell kinetic model of granulopoiesis under radiation exposure: Extension from rodents to canines and humans. Radiat Prot Dosimetry 143(2-4):207-213

Hu S, Cucinotta FA (2011b) Characterization of the Radiation-Damaged Precursor Cells in Bone Marrow Based on Modeling of the Peripheral Blood Granulocytes Response. Health Phys 101(1):67-78 2011

Hu S, Smirnova OA, Cucinotta FA (2012) A biomathematical model of lymphopoiesis following severe radiation accidents--potential use for dose assessment. Health Phys 102(4):425-436

Hu S, Cucinotta FA (2013) Modeling the depressed hematopoietic cells for immune system under chronic radiation. In Computational Intelligence Methods for Bioinformatics and Biostatistics, Lecture Notes in Computer Science 7845:26-36

Hu S, Cucinotta FA (2014) Epidermal homeostasis and radiation responses in a multiscale tissue modeling framework. Integr Biol 6:76-89

ICRP (2000) Avoidance of Radiation Injuries from Medical Interventional Procedures. ICRP Publication No 85, Ann ICRP 30(2)

ICRP (2002) Prevention of Accidents to Patients Undergoing Radiation Therapy. ICRP Publication No 86, Ann ICRP 30(3)

ICRP (2007) The 2007 Recommendations of the International Commission on Radiological Protection. ICRP Publication No 103, Ann ICRP 37 (2/4)

ICRP (2012) ICRP Statement on Tissue Reactions / Early and Late Effects of Radiation in Normal Tissues and Organs – Threshold Doses for Tissue Reactions in a Radiation Protection Context. ICRP Publication 118, Ann ICRP 41(1/2)

Iglesias-Bartolome R, Patel V, Cotrim A, Leelahavanichkul K, Molinolo AA, Mitchell JB, Gutkind JS (2012) mTOR inhibition prevents epithelial stem cell senescence and protects from radiation-induced mucositis. Cell Stem Cell 11(3):401-414

Ishida M, Matsubayashi I (1948) An analysis of early mortality rates following the atomic bomb of Hiroshima. Radiation Effects Research Foundation, Atomic Bomb Casualty Commissions, Hiroshima, Japan, pp. 20–61

Jia D, Koonce NA, Griffin RJ, Jackson C, Corry PM (2010) Prevention and Mitigation of Acute Death of Mice after Abdominal Irradiation by the Antioxidant N-Acetyl-cysteine (NAC). Radiat Res 173(5):579–589

Jiggens PT, Gabriel SB, Heynderickx AH, Crosby N, Glover, A, Hilgers A (2012) ESA SEPEM Project: Peak Flux and Fluence Model. IEEE Trans Nucl Sci 59:1066-1077

Jones TD (1981) Hematologic syndrome in man modeled from mammalian lethality. Health Phys 41:83–103

Kang A, Cosenza S, Bonagura M, Manair M, Reddy M, Reddy E (2013) ON01210.Na (Ex-RAD®) mitigates radiation damage through activation of the AKT pathway. PLOS One 8(3):e58355

Kantara C, Moya SM, Houchen CW, Umar S, Ullrich RL, Singh P, Carney DH (2015) Novel regenerative peptide TP508 mitigates radiation-induced gastrointestinal damage by activating stem cells and preserving crypt integrity. Lab Invest 95(11):1222-1233

Kase PG (1970) Computerized anatomical model man. Technical Report, AD-868927, MCR-69-409, AFWL-TR-69-161, Contract F29601-69-C-0052. Martin Marietta Corp, Denver, CO

Kennedy AR, Todd P (2003) Biological countermeasures in space radiation health. Gravit Space Biol Bull 16(2):37-44

Kennedy AR, Zhou Z, Donahue JJ, Ware JH (2006) Protection against adverse biological effects induced by space radiation by the Bowman-Birk inhibitor and antioxidants. Radiat Res 166(2):327-332

Kennedy AR, Davis JG, Carlton W, Ware JH (2008) Effects of Dietary Antioxidant Supplementation on the Development of Malignant Lymphoma and Other Neoplastic Lesions in Mice Exposed to Proton or Iron-Ion Radiation Radiat Res 169:615–625

Kennedy AR, Wan XS (2011) Countermeasures for space radiation induced adverse biologic effects. Adv Space Res 48(9):1460-1479

Kennedy AR (2014) Biological Effects of Space Radiation and Development of Effective Countermeasures Life Sci Space Res 1:10–43

Kim J, Kolozsvary A, Jenrow K, Brown S (2012) Plerixafor, a CXCR4 antagonist, mitigates skin radiation-induced injury in mice. Radiat Res 178:202-206

Kim MY, Wilson JW, Simonsen LC, Cucinotta FA, Atwell W, Badavi FF, Miller J (1999) Contribution of High Charge and Energy (HZE) Ions During Solar-Particle Event of September 19, 1989. NASA TP-1999-209320

Kim M.Y., Hu X, Cucinotta FA (2005) Effect of Shielding Materials from SPEs on the Lunar and Mars Surface. AIAA Space 2005, AIAA-2005-6653

Kim MY, Cucinotta FA, Wilson JW (2006) Mean occurrence frequency and temporal risk analysis of solar particle events. Radiat Meas. 41:1115–1112

Kim MY, Hayat MJ, Feiveson AH, Cucinotta FA (2009a) Prediction of frequency and exposure level of solar particle events. Health Phys 97:68-81

Kim MY, Hayat MJ, Feiveson AH, Cucinotta FA (2009b) Using High-Energy Proton Fluence to Improve Risk Prediction for Consequences of Solar Particle Events. Adv Space Res 44(12):1428-1432

Kim K, Pollard JM, Norris AJ et al (2009) High-Throughput Screening Identifies Two Classes of Antibiotics as Radioprotectors: Tetracyclines and Fluoroquinolones. Clin Cancer Res 15:7238

Kim MY, Hu S, Nounu HN, Cucinotta FA (2010) Development of Graphical User Interface for ARRBOD (Acute Radiation Risk and BRYNRN Organ Dose Projection. NASA/TP-2010-216116

Kim MY, De Angelis G, Cucinotta FA (2011) Probabilistic Assessment of Radiation Risk for Astronauts in Space Missions. Acta Astronautica 68:747-759

King GL, Rabin BM, Weatherspoon JK (1999) 5-HT3 receptor antagonists ameliorate emesis in the ferret evoked by neutron or proton radiation. Aviat Space Environ Med 70:485–492

King JH (1974) Solar proton fluences from 1977-1983 space missions. J Spacecraft 11(6):401-408

Kodaira M, Satoh C, Hiyama K, Toyama K (1995) Lack of effects of atomic bomb radiation on genetic instability of tandem-repetitive elements in human germ cells. Am J Hum Genet 57(6):1275-1283

Kovalev EE, Smirnova OA (1996) Estimation of radiation risk based on the concept of individual variability of radiosensitivity. AFRRI Contract Report 96-1

Kovaltsov GA, Usoskin IG (2014) Occurrence probability of large solar energetic particle events: Assessment from data on cosmogenic radionuclides in lunar rocks. Solar Phys 289:211-220

Kozarev K, Schwadron NA, Dayeh MA et al (2010) Modeling the 2003 Halloween events with EMMREM: Energetic particles, radial gradients, and coupling to MHD. Space Weather 8: S00E08

Krigsfeld GS, Sanzari J, and Kennedy AR (2012) The effects of proton radiation on the prothrombin and partial thromboplastin times of irradiated ferrets. Int J Radiat Biol 88(4):327-334

Krigsfeld GS, Savage AR, Sanzari JK, Wroe AJ, Gridley DS, Kennedy AR (2013a) Mechanism of hypocoagulability in proton irradiated ferrets. Int J Radiat Biol 89(10):823-831

Krigsfeld GS, Kennedy AR (2013b) Is disseminated intravascular coagulation the major cause of mortality from radiation at relatively low whole body doses? Radiat Res 180(3):231-234

Kulkarni S, Singh PK, Ghosh SP, Posarac A, Singh VK (2013) Granulocyte colony-stimulating factor antibody abrogates radioprotective efficacy of gamma-tocotrienol, a promising radiation countermeasure. Cytokine 62(2):278-285

Kumar D, Salian SR, Kalthur G et al (2013) Semen abnormalities, sperm DNA damage and global hypermethylation in health workers occupationally exposed to ionizing radiation. PLoS One. 8(7):e69927

Langell J, Jennings R, Clark J, Ward J (2008) Pharmacological agents for the prevention and treatment of toxic radiation exposure in spaceflight. Aviat Space Environ Med 79(7):651-660

Lario D, Kallenrode MB, Decker RB et al (2006) Radial and Longitudinal Dependence of Solar 4-13 MeV and 27-37 MeV Proton Peak Intensities and Fluences: Helios and IMP 8 Observations. Astrophys J 653(2):1531-1544

Lazo JS, Sharlow ER, Epperly MW, Lira A, Leimgruber S, Skoda EM, Wipf P, Greenberger JS (2013) Pharmacologic Profiling of Phosphoinositide 3-Kinase Inhibitors as Mitigators of Ionizing Radiation–Induced Cell Death. JPET 347(3):669-680

Li XH, Ha CT, Fu D, Landauer MR, Ghosh SP, Xiao M (2015) Delta-Tocotrienol Suppresses Radiation-Induced MicroRNA-30 and Protects Mice and Human CD34+ Cells from Radiation Injury. PLoS ONE 10(3):e0122258

Limoli CL, Giedzinski E, Baure J, Rola R, Fike JR (2007) Redox changes induced in hippocampal precursor cells by heavy ion irradiation. Radiat Environ Biophys 46(2):167-172

Livshits LA, Malyarchuk SG, Kravchenko SA et al (2001) Children of Chernobyl cleanup workers do not show elevated rates of mutations in minisatellite alleles. Radiat Res 155(1 Pt 1):74-80

Loria R, Beckman M, Contaifer D, Tamariz F, Gibb D, Thompson L, Guida P (2011) Beta androstenediol mitigates the damage of 1 GeV/n Fe ion particle radiation to the hematopoietic system. Cancer Biother Radiopharma 26(4):453-459

Lushbaugh CC (1962) What can we expect to happen? Rocky Mt Med J 59:37-50

Lushbaugh CC (1969) Reflections on some recent progress in human radiobiology. Adv Radiat Biol 3:277–315

Lushbaugh CC (1974) Human radiation tolerances In: Tobias CA, Todd P (eds) Space Radiation and Related Topics, Academic Press, NY

Maks CJ, Wan XS, Ware JH et al (2011) Analysis of white blood cell counts in mice following gamma or proton radiation exposure. Radiat Res 176:170-176

Marshburn TH (2008) Acute Care In: Barratt MR, Pool SL (eds) Principles of Clinical Medicine for Space Flight, Springer, NY pp 101-122

Matheson LN, Dore MA, Anno GH, McClellan GE (1995) User's manual: radiation-induced performance decrement (RIPD), version 2.0. Alexandria, VA: Defense Nuclear Agency; DNA-TR-95-91

McFarland W, Pearson HA (1963) Hematological events as dosimeters in human total-body irradiation. Radiol 80:850–855

McKracken KG, Dreschhoff G, Zeller EJ, Smart DF, Shea MA (2001) Solar cosmic ray events for the period 1561–1994 1. Identification in polar ice, 1561–1950. J Geophys Res 106(A10):21585–21598

Mehrotra S, Pecaut M, Gridley D (2012) Analysis of minocycline as a countermeasure against acute radiation syndrome. In Vivo 26:743-758

Meistrich ML. (2013) Effects of chemotherapy and radiotherapy on spermatogenesis in humans. Fertil Steril 100(5):1180-1186

Messerschmidt O (1979) Medical procedures in a nuclear disaster. Verlag-Karl Thieming, Munich, Federal Republic of Germany, pp 95–115

Mettler F (2012) Medical effects and risks of exposure to ionising radiation. J Radiol Prot 32:N9-N13

Miller AD, Leslie RA (1994) The area postrema and vomiting. Front Neuroendocrinol 15:301-320

Montagna W, Yun JS (1964) The skin of the domestic pig. J Invest Dermatol 42:11-21

Musgrave GE, Larson AM, Sgobba T (2009) Safety Design for Space Systems. Elsevier Burlington MA, pp 53-38

Nakamura N (2006) Genetic effects of radiation in atomic-bomb survivors and their children: past, present and future. J Radiat Res 47(Suppl B):B67-73

NASA (2007) National Aeronautics and Space Administration. NASA Space Flight Human System Standard. Volume 1: Crew Health. NASA Technical Standard NASA-STD-3001

NASA (2011) National Aeronautics and Space Administration. NASA Space Flight Human System Standard. Volume 2: Human Factors, Habitability, And Environmental Health. NASA Technical Standard NASA-STD-3001

NASA (2014) National Aeronautics and Space Administration. NASA Space Flight Human System Standard. Volume 1, Revision A: Crew Health. NASA Technical Standard NASA-STD-3001

NAS/NRC (1967) Radiobiological factors. In: Langham WH (ed) Manned Spaceflight, Report of Space Radiation Study Panel of the Life Sciences Committee, National Academy Press, Washington, DC

NAS/NRC (1970) Radiation Protection Guides and Constraints for Space-Mission and Vehicle-Design Studies Involving Nuclear Systems. National Academy Press, Washington, DC

NAS/NRC (2006) Space Radiation Hazards and the Vision for Space Exploration. National Academy Press, Washington. DC

NCRP (1982) The Control of Exposure of the Public to Ionizing Radiation in the Event of an Accident or Attack. Proceedings of a Symposium held on April 26–28, 1981. NCRP, Bethesda, MD

NCRP (1989a) Guidance on Radiation Received in Space Activities. NCRP Report No 98, NCRP, Bethesda, MD

NCRP (1989b) Limit for exposure to hot particles on the skin. NCRP Report No 106, NCRP, Bethesda, MD

NCRP (1993) Limitation of Exposure to Ionizing Radiation. NCRP Report No 116, NCRP, Bethesda, MD

NCRP (2000) Recommendations of Dose Limits for Low Earth Orbit. NCRP Report No 132, NCRP, Bethesda, MD

NCRP (2006) Information Needed To Make Radiation Protection Recommendations for Space Missions Beyond Low-Earth Orbit. NCRP Report No 153, NCRP, Bethesda, MD

Neel JV, Schull WJ, Awa AA, Satoh C, Kato H, Otake M, Yoshimoto Y (1990) The children of parents exposed to atomic bombs: estimates of the genetic doubling dose of radiation for humans. Am J Hum Genet 46(6):1053-1072

Nitta Y, Hoshi M (2003) Relationship between oocyte apoptosis and ovarian tumours induced by high and low LET radiations in mice. Int J Radiat Biol 79(4):241-250

NRC (2008) Managing space radiation risk in the new era of space exploration. National Academies Press, Washington, DC

Nomura T, Nakajima H, Ryo H, Li LY, Fukudome Y, Adachi S, Gotoh H, Tanaka H (2004) Transgenerational transmission of radiation- and chemically induced tumors and congenital anomalies in mice: studies of their possible relationship to induced chromosomal and molecular changes. Cytogenet Genome Res 104(1-4):252-260

Ni H, Balint K, Zhou Y, Gridley DS, Maks C, Kennedy AR, Weissman D (2011) Effect of solar particle event radiation on gastrointestinal tract bacterial translocation and immune activation. Radiation Res 175(4):485-492

Nymmik R (1999) Probabilistic model for fluences and peak fluxes of solar energetic particles. Radiat Measur 30:287–296

Ogilvy-Stuart AL, Shalet SM (1993) Effect of radiation on the human reproductive system. Environ Health Perspect 101(Suppl 2):109-116

Ohkita II T (1975) A review of thirty years of study of Hiroshima and Nagasaki atomic bomb survivors. J Radiat Res 16(Suppl):49–66

Okunieff P, Xu J, Hu D, Liu W, Zhang L, Morrow G, Pentland A, Ryan JL, Ding I (2006) Curcumin protects against radiation-induced acute and chronic cutaneous toxicity in mice and decreases mRNA expression of inflammatory and fibrogenic cytokines. Int J Radiat Oncol Biol Phys 65(3):890-898

Oughterson AW, Warren S (1956) Medical effects of the atomic bomb in Japan. McGraw-Hill Book Company, NY

Parsons JL, Townsend LW (2000) Interplanetary Crew Dose Rates for the August 1972 Solar Particle Event. Radiat Res 153:729-733

Paulsen CA (1973) The study of irradiation effects on the human testes: Including histologic, chromosomal and hormonal aspects. Terminal Report, AEC contract AT(45-1)-2225. National Technical Information Service, Springfield, VA

Paunesku D, Paunesku T, Wahl A, Kataoka Y, Murley J, Grdina DJ, Woloschak GE (2008) Incidence of tissue toxicities in gamma ray and fission neutron-exposed mice treated with Amifostine. Int J Radiat Biol 84(8):623-634

Peebles D, Soref C, Copp R, Thunberg A, Fahl W (2012) ROS-Scavenger and radioprotective efficacy of the new PrC-210 aminothiol. Radiat Res 178(1):57-68

Pellmar RC, Rockwell S et al (2005) Priority list of research areas for radiological nuclear threat countermeasures. Radiat Res 163:115–123

Rabin BM, Hunt WA, Wilson ME, Josepha JA (1992) Emesis in ferrets following exposure to different types of radiation: A dose-response study. Aviat Space Environ Med 63:702–705

Rabin BM, Joseph JA, Hunt WA, Dalton TB, Kandasamy SB, Harris AH, Ludewigt B (1994) Behavioral endpoints for radiation injury. Adv Space Res 14:457–466

Rabin BM, Shukitt-Hale B, Joseph J, Todd P (2005) Diet as a factor in behavioral radiation protection following exposure to heavy particles. Gravit Space Biol Bull 18(2):71-77

Ramakrishnan N, Wolfe WW, Catravasg GN (1992) Radioprotection of Hematopoietic Tissues In Mice By Lipoic Acid. Radiat Res 130:360-365

Ran Y, Wang R, Gao Q et al (2014) Dragon's blood and its extracts attenuate radiation-induced oxidative stress in mice. J Radiat Res 55(4):699-706

Reames D (1999) Solar energetic particles: Is there time to hide? Radiat Measur 30:297-308

Romero-Weaver AL, Wan XS, Diffenderfer ES, Lin L, Kennedy AR (2013) Effect of SPE-like proton and photon radiation on the kinetics of mouse peripheral blood cells and radiation biological effectiveness determinations. Astrobiology 13:570-577

Romero-Weaver AL, Wan XS, Diffenderfer ES, Lin L, Kennedy AR (2013) Kinetics of Neutrophils in Mice Exposed to Radiation and/or Granulocyte Colony-Stimulating Factor Treatment. Radiat Res 80(2):177-188

Romero-Weaver AL, Ni J, Lin L, Kennedy AR (2014) Orally Administered Fructose Increases the Numbers of Peripheral Lymphocytes Reduced by Exposure of Mice to Gamma or SPE-like Proton Radiation. Life Sci Space Res 2:80–85

Rosen EM, Day R, Singh VK (2015) New Approaches to Radiation Protection. Front Oncol 4:381

Rotolo J, Stancevic B, Zhang J, Hua G, Fuller J, Yin X et al (2012) Anti-ceramide antibody prevents the radiation gastrointestinal syndrome in mice. J Clin Invest 122(5):1786-1790

Ryan JL, Carroll JK, Ryan EP, Mustian KM, Fiscella K, Morrow GR (2007) Mechanisms of cancer-related fatigue. The Oncologist 12(suppl 1):22-34

Ryan J (2012) Ionizing radiation: the good, the bad, and the ugly. J Invest Dermatol 132:985-993

Ryan J, Heckler C, Ling M, Katz A, Williams J, Pentland A, Morrow G (2013) Curcumin for radiation dermatitis: a randomized, double-blind, placebo-controlled clinical trial of thirty breast cancer patients. Radiat Res 180(1):34-43

Sachs L (1996) The control of hematopoiesis and leukemia: from basic biology to the clinic. Proc Natl Acad Sci USA 93:4742– 4749

Samarth RM, Kumar A (2003) Radioprotection of Swiss albino mice by plant extract Mentha piperita (Linn.). J Radiat Res 44(2):101-109

Sanzari JK, Wambi C, Lewis-Wambi JS, Kennedy AR (2011) Antioxidant dietary supplementation in mice exposed to proton radiation attenuates expression of programmed cell death-associated genes. Radiat Res 175(5):650-656

Sanzari JK, Wan XS, Wroe AJ, Rightnar S, Cengel KA, Diffenderfer ES, Krigsfeld GS, Gridley DS, Kennedy AR (2013a) Acute hematological effects of solar particle event proton radiation in the porcine model. Radiat Res. 180(1):7-16

Sanzari JK, Wan XS, Krigsfeld GS et al (2013b) Effects of solar particle event proton radiation on parameters related to ferret emesis. Radiat Res 180(2):166-176

Sanzari JK, Wan XS, Krigsfeld GS, Wroe AJ, Gridley DS, Kennedy AR (2013c) The effects of gamma and proton radiation exposure on hematopoietic cell counts in the ferret model. Gravitat Space Biol 1(1):79-94

Sanzari JK, Romero-Weaver AL, James G, Krigsfeld G, Lin L, Diffenderfer ES, Kennedy AR (2013d) Leukocyte activity is altered in a ground based murine model of microgravity and proton radiation exposure. PLoS One 8(8):e71757

Sanzari JK, Wan XS, Diffenderfer ES, Cengel KA, and Kennedy AR (2014) Relative biological effectiveness of simulated solar particle event proton radiation to induce acute hematological change in the porcine model. J Radiat Res 55(2): 228–244

Sanzari JK, Krigsfeld GS, Shuman AL, Diener AK, Lin L, Mai W, Kennedy AR (2015) Effects of a granulocyte colony stimulating factor, Neulasta, in mini pigs exposed to total body proton irradiation. Life Sci Space Res 5:13-20

Sapp WJ, Philpott DE, Williams CS, Williams JW, Kato K, Miquel JM, Serova L (1992) Comparative study of spermatogonial survival after x-ray exposure, high LET (HZE) irradiation or spaceflight. Adv Space Res 12(2-3):179-89

Sato T, Kinoshita M, Yamamoto T, Ito M, Nishida T, Takeuchi M et al (2015) Treatment of Irradiated Mice with High-Dose Ascorbic Acid Reduced Lethality. PLoS ONE 10(2): e0117020

Satyamitra M, Lombardini E, Graves J III et al (2011) A TPO Receptor Agonist, ALXN4100TPO, Mitigates Radiation-Induced Lethality and Stimulates Hematopoiesis in CD2F1 Mice. Radiat Res 175:746–758

Scarantino CW, Ornitz RD, Hoffman LG, Anderson RF Jr. (1994) On the mechanism of radiation-induced emesis: the role of serotonin. Int J Radiat Oncol Biol Phys 30(4):825-830

Schaefer HJ (1957) Cosmic-ray dosage during the giant solar flare of February 23, 1956, J Aviat Med 28:387-396

Schmiegelow M, Feldt-Rasmussen U, Rasmussen AK et al (2003) Assessment of the hypothalamo–pituitary–adrenal axis in patients treated with radiotherapy and chemotherapy for childhood brain tumor. J Clin Endocrinol Metab 88:3149–3154

Schover LR (2005) Sexuality and fertility after cancer. Hematolology Am Soc Hematol Educ Program 5:523-527

Schrijver CJ, Beer J, Baltensperger U et al (2012) Estimating the frequency of extremely energetic solar events, based on solar, stellar, lunar, and terrestrial records. J Geophys Res 117(A8): A017706

Schwadron N, Townsend L, Kozarev K et al (2010) Earth-Moon-Mars Radiation Environment Module Framework. AGU Space Weather Journal 8:S00E02

Serin M, Gülbaş H, Gürses I, Erkal HS, Yücel N (2007) The histopathological evaluation of the effectiveness of melatonin as a protectant against acute lung injury induced by radiation therapy in a rat model. Int J Radiat Biol 83(3):187-193

Shalit I, Kletter Y, Weiss K, Gruss T, Fabian I (1997) Enhanced hematopoiesis in sublethally irradiated mice treated with various quinolones. Eur J Haematol 58(2):92-98

Shea MA, Smart DF (1990) A summary of major proton events. Solar Phys 127:297–320

Simon MA, Clowdsley MS, Walker SA (2013) Habitat Design Considerations for Implementing Solar Particle Event Radiation Protection. Proceedings of the 43rd International Conference on Environmental Systems, Vail, CO, USA, July 14-18. AIAA 2013-3402

Sine RC, Levine IH, Jackson WE, Hawley AL, Prasanna PG, Grace MB, Goans RE, Greenhill RG, Blakely WF (2001) Biodosimetry Assessment Tool: a post-exposure software application for management of radiation accidents. Mil Med 166(12 Suppl):85-87

Singh VK, Christensen J, Fatanmi OO, Gille D, Ducey EJ, Wise SY, Karsunky H, Sedello AK (2012) Myeloid progenitors: a radiation countermeasure that is effective when initiated days after irradiation. Radiat Res 177(6):781-791

Singh V, Beattie L, Seed T (2013) Vitamin E: tocopherols and tocotrienols as potential radiation countermeasures. J Radiat Res 54:973-988

Singh VK, Newman VL, Romaine PL, Wise SY, Seed TM (2014) Radiation countermeasure agents: an update (2011-2014). Expert Opin Ther Pat 24(11):1229-1255

Singh V, Wise S, Scott JR, Romaine PLP, Newman VL, Fatanmi OO (2014) Radioprotective efficacy of delta-tocotrienol, a vitamin E isoform, is mediated through granulocyte colony-stimulating factor. Life Sci 98:113–122

Singh VK, Romaine PLP, Newman VL (2015) Biologics as countermeasures for acute radiation syndrome: where are we now? Expert Opin Biol Ther 15(4):465-471

Singleterry RC, Blattnig S, Clowdsley MS et al (2010) OLTARIS: On-Line Tool for the Assessment of Radiation in Space. NASA/TP-2-1—216722

Smart DF, Shea MA (2003) Comment on estimating the solar proton environment that may affect Mars missions. Adv Space Res 31(1):45-50

Smirnova OA (1999) Mathematical models of hematopoiesis dynamics in nonirradiated and irradiated mammals. In: BioMedSim'99, Proceedings of the 1st conference on modelling and simulation in biology, medicine and biomedical engineering. Paris: Groupe ESIEE 105–109

Smirnova OA, Yonezawa M (2003) Radioprotection effect of low level preirradiation on mammals: modeling and experimental investigations. Health Phys 85:150 –158

Smirnova OA, Yonezawa M (2004) Radioresistance in mammals induced by low-level chronic irradiation: modeling and experimental investigations. Health Phys. 87(4):366–374

Smirnova OA (2009) Blood and small intestine cell kinetics under radiation exposures: Mathematical modeling. Adv Space Res 44:1457-1469

Smirnova OA (2011) Environmental radiation effects on mammals: a dynamical modeling approach. Springer, New York

Smirnova OA (2012) Comparative analysis of the dynamics of thrombocytopoietic, granulocytopoietic, and erythropoietic systems in irradiated humans: a modeling approach. Health Phys 103:787-801

Smirnova OA, Hu S, Cucinotta FA (2014) Dynamics of acutely irradiated skin epidermal epithelium in swine: modeling studies. Health Phys 107(1):47-59

Soligenix http://www.soligenix.com/pipeline/vaccinesbiodefense/orbeshield-for-gastrointestinal-acute-radiation-syndrome-gi-ars/

Soref C, Hacker T, Fahl W (2011) A new orally active, aminothiol radioprotector-free of nausea and hypotension side effects at its highest radioprotective doses. Int J Radiation Oncol Biol Phys 82(5):e701-e707

Steinbach KH, Raffler H, Pabst G, Fliedner TM (1980) A mathematical model of canine granulocytopoiesis. J Math Biol 10:1–12

Stickney DR, Dowding C, Garsd A, Ahlem C, Whitnall M, McKeon M, Reading C, Frinck J (2006) 5-androstenediol stimulates multilineage hematopoiesis in rhesus monkeys with radiation-induced myelosuppression. Int Immunopharmacol 6(11):1706-1713

Stodtmeister R, Sandkühler S, Fliedner TM (1956) Über die Pathogenese akuter Knochenmarkatrophie bei Ratten nach Ganzkörperbestrahlung mit schnellen Elektronen. Folia Haematologica 3:303–345

Stone H, Moulder J, Coleman C et al (2004) Models for evaluating agents intended for the prophylaxis, mitigation and treatment of radiation injuries. Report of an NCI Workshop, December 3-4, 2003. Radiat Res 162(6):711-28

Strom DJ (2003) Health impacts from acute radiation exposure. Pacific Northwest National Laboratory Report PNNL-14424, Richland, Washington

Strominger NL, Knox AP, Carpenter DO (1994) The connectivity of the area postrema in the ferret. Brain Res Bull 33:33-47

Sureban SM, May R, Qu D et al (2015) Dietary Pectin Increases Intestinal Crypt Stem Cell Survival following Radiation Injury. PLoS ONE 10(8):e0135561

Tahamtan R, Shabestani Monfared A, Tahamtani Y, Tavassoli A, Akmali M, Mosleh-Shirazi MA (2015) Radioprotective effect of melatonin on radiation-induced lung injury and lipid peroxidation in rats. Cell J 17(1):111-120

Thomas LJ, JM, Round SM, Naylor SR, Forsberg EM, Borrelli KM, Pilsmaker CD, Gergel LE, Marsh HC, Keler T (2013) Radioprotective and Radiomitigative Efficacy of Flt3 Ligand in a Murine Model of Acute Radiation Injury. The FASEB Journal 27:1181.3

Tikka T, Fiebich BL, Goldsteins G, Keinanen R, Koistinaho J (2001) Minocycline, a tetracycline derivative, is neuroprotective against excitotoxicity by inhibiting activation and proliferation of microglia. J Neurosci 21(8):2580-2588

Till JE and McCulloch EA (1961) A direct measurement of the radiation sensitivity of normal mouse bone marrow cells. Radiat Res 14:213-222

Townsend LW, Cucinotta FA, Wilson JW, Bagga R (1994) Estimates of HZE Particle Contributions to SPE Radiation Exposures on Interplanetary Missions. Adv Space Res 10:671–674

Tylka AJ, Dietrich WF (2009) A New Comprehensive Analysis of Proton Spectra in Ground-Level Enhanced (GLE) Solar Particle Events. Proceedings of the 31st International Cosmic Ray Conference, Lodz, Poland, July 7-15

UNSCEAR (2001) United Nations Scientific Committee on the Effects of Atomic Radiation. Hereditary Effects of Radiation. The 2002 Report to the General Assembly with Scientific Annex. New York: United Nations 2001

Vanamala J, Glagolenko A, Yang P et al (2008) Dietary fish oil and pectin enhance colonocyte apoptosis in part through suppression of PPARdelta/PGE2 and elevation of PGE3. Carcinogenesis 29(4):790-796

Vasin MV, Semenov LF, Suvorov NN, Antipov VV, Ushakov IB, Ilyin LA, Lapin BA (2014) Protective effect and the therapeutic index of indralin in juvenile rhesus monkeys. J Radiat Res 55(6):1048-1055

Verkhoglyadova OP, Li G, Ao X, Zank GP (2012) Radial dependence of peak proton and iron ion fluxes in solar energetic particle events: Application of the PATH code. Astrophys J 757:75-83

Vodopick H, Andrews GA (1974) Accidental radiation exposure. Arch Environ Health 28:53–56

Walker SA, Clowdsley MS, Abston HL, Simon MA, Gallegos AM (2013) Radiation Exposures Analysis Supporting the Development of Solar Particle Shielding Technologies. Proceedings of the 43rd International Conference on Environmental Systems, Vail, CO, USA, July 14-18. AIAA 2013-3402

Wallace WH, Thomson AB, Kelsey TW (2003) The radiosensitivity of the human oocyte. Hum Reprod 18(1):117-21

Wambi C, Sanzari J, Wan XS et al (2008) Dietary antioxidants protect hematopoietic cells and improve animal survival after total-body irradiation. Radiat Res 169(4):384-396

Wambi CO, Sanzari JK, Sayers CM et al (2009) Protective effects of dietary antioxidants on proton total-body irradiation-mediated hematopoietic cell and animal survival. Radiat Res 172(2):175-186

Wang SC, Borison HL (1950) The vomiting center: a critical experimental analysis. Arch Neurol Psychiatry 63:928-41

Ware JH, Sanzari J, Avery S, Sayers C, Krigsfeld G, Nuth M, Wan XS, Rusek A, Kennedy AR (2010). Effects of proton radiation dose, dose rate and dose fractionation on hematopoietic cells in mice. Radiat Res 174:325-330

Warren S, Grahn D (1973) Ionizing radiation. In: Parker J Jr, West VR (eds) Bioastronautics data book, NASA TP-3006

Waselenko JK, MacVittie TJ, Blakely WF et al (2004). Medical Management of the Acute Radiation Syndrome: Recommendations of the Strategic National Stockpile Radiation Working Group. Ann Intern Med 140:1037-1051

Whitnall M (2012) Mitigating Radiation Adverse Effects: State of the Art and Challenges. In: Proceedings of NATO RTO HFM-223 Symposium Biological Effects of Ionizing Radiation Exposure and Countermeasures: Current Status and Future Perspectives, Slovenia 2012

Whitnall MH, Villa V, Seed TM, Benjack J, Miner V, Lewbart ML, Dowding CA, Jackson WE (2005) Molecular specificity of 5-androstenediol as a systemic radioprotectant in mice. Immunopharmacol Immunotoxicol 27(1):15-32

Wichmann HE, Loeffler M (1985) Mathematical modeling of cell proliferation: stem cell regulation in hemopoiesis. CRC Press, Boca Raton

Wilson JW, Townsend LW, Nealy JE et al (1989) BRYNTRN: A Baryon transport model. Washington DC, NASA Report No. TP-2887

Wilson JW, Cucinotta FA, Jones TD, Chang CK (1997) Astronaut protection from solar event of August 4, 1972. Hanover, MD: Center for Aerospace Information; NASA-TP 3643

Wilson JW, Cucinotta FA, Kim M, Shinn JL, Jones TD, Chang CK (1999) Biological Response to SPE Exposure. Radiat Meas 30:361–370

Wilson JW, Kim MY, De Angelis G, Cucinotta FA, Yoshizawa N, Badavi FF (2002) Implementation of Gy-Eq for deterministic effects limitation in shield design. J. Radiat Res 43:S103-S106

Wilson JW, Cucinotta FA, Golightly MJ et al (2006) International space station: A testbed for experimental and computational dosimetry. Adv Space Res 37:1656-1663

Wilson JM, Diffenderfer ES, Sanzari JK et al (2011) Acute biological effects of simulating the whole body radiation dose distribution from a solar particle event in a porcine model. Radiat Res 176(5):649-659

Wilson JM, Krigsfeld GS, Sanzari JK, Wagner EB, Mick R, Kennedy AR (2012) Comparison of hindlimb unloading and partial weight suspension models for spaceflight-type condition induced effects on white blood cells. Adv Space Res 49:237-248

Xapsos MA, Barth JL, Stassinopoulos EG, Burke EA, Gee GB (1999) Space environment effects: Model for emission of solar protons (ESP): Cumulative and worst case event fluences. NASA TP 209763

Xapsos M, Summers G, Barth J, Stassinopoulos E, Burke E. (2000) Probability model for cumulative solar proton event fluences. IEEE Transactions Nucl Sci (47):486–490

Xapsos MA, Stauffer C, Gee GB, Barth JL, Stassinopoulos EG, McGuire RE (2004) Model for solar proton risk assessment. IEEE Trans Nucl Sci 51:3394–3398

Xapsos MA, Stauffer C, Jordon T, Barth JL, Mewaldt RA (2007) Model for Cumulative Solar Heavy Ion Energy and Linear Energy Transfer Spectra. IEEE NSREC07 B-4

Xiao M, Whitnall MH (2009) Pharmacological Countermeasures for the Acute Radiation Syndrome. Curr Mol Pharmacol 2:122-133

Xin N, Li Y, Li X et al (2012) Dragon's Blood May Have Radioprotective Effects in Radiation-Induced Rat Brain Injury. Radiat Res 178 (1):75-85

Xu L, Xiong S, Guo R, Yang Z, Wang Q, Xiao F, Wang H, Pan X, Zhu M (2014) Transforming growth factor β3 attenuates the development of radiation-induced pulmonary fibrosis in mice

by decreasing fibrocyte recruitment and regulating IFN-γ/IL-4 balance. Immunol Lett 162(1 Pt A):27-33
Yarbro CH, Perry MC (1985) The effect of cancer therapy on gonadal function. Semin Oncol Nurs 1(1):3-8
Yang TC (1999) Proton radiobiology and uncertainties. Radiat Meas 30:383-392
Yucker WR, Huston SL (1990) Computerized Anatomical Female. Report MDC H 6107, McDonnell Douglas Corporation, Huntington Beach, CA, September 1990
Yucker WR (1992) Computerized Anatomical Female Body Self-Shielding Distributions. Report MDC 92H0749, McDonnell Douglas Corporation, Huntington Beach, CA, March 1992
Zagon A, Totterdell S, Jones RS (1994) Direct projections from the ventrolateral medulla oblongata to the limbic forebrain: anterograde and retrograde tract-tracing studies in the rat. J Comp Neurol 340:445-468
Zellefrow CD, Sharlow ER, Epperly MW, Reese CE, Shun T, Lira A, Greenberger JS, Lazo JS (2012) Identification of Druggable Targets for Radiation Mitigation Using a Small Interfering RNA Screening Assay. Radiat Res 178 (3)150-159
Zhang R, Burns FJ, Chen H, Chen S, Wu F (2006) Alterations in Gene Expression in Rat Skin Exposed to 56Fe Ions and Dietary Vitamin A Acetate. Radiat Res 165:570–581
Zhang K, Tian Y, Yin L, Zhang M, Beck LA, Zhang B, Okunieff P, Zhang L, Vidyasagar S (2011) Fibroblast growth factor-peptide improves barrier function and proliferation in human keratinocytes after radiation. Int J Radiat Oncol Biol Phys 81(1):248-254
Zhou Y, Ni H, Li M, Sanzari JK, Diffenderfer ES, Lin L, Kennedy AR, Weissman D (2012) Effect of solar particle event radiation and hindlimb suspension on gastrointestinal tract bacterial translocation and immune activation. PLoS ONE 7(9):e44329
Zukhbaya TM, Smirnova OA (1991) An experimental and mathematical analysis of lymphopoiesis dynamics under continuous irradiation. Health Phys 60:87–95

X. Team

Steve Blattnig, PhD, is a scientist at NASA Langley Research Center, Hampton, VA. He is the Principal Investigator for the SRPE Risk Assessment Project.

Lisa Carnell, PhD, is a scientist at NASA Langley Research Center, Hampton, VA, and is the Space Radiation Program Element Biological Countermeasures Lead across all risks.

Shaowen Hu, PhD, is a scientist with the Wyle Science, Technology and Engineering group based in Houston, TX. His work focuses on development of ARRBOD risk models for prediction of health effects from SPEs.

Janice Huff, PhD, is a senior scientist with Universities Space Research Association, Houston, TX, and is the NASA Space Radiation Program Element Deputy Element Scientist.

Myung-Hee Kim, PhD, is a senior scientist with the Wyle Science, Technology and Engineering group based in Houston, TX. She is a developer of SPE models and a lead for integration of radiation transport codes and risk models.

Ryan Norman, PhD, is a scientist at NASA Langley Research Center, Hampton, VA.

Zarana Patel, PhD, is a senior scientist with Wyle Science, Technology and Engineering Group based in Houston, TX and is the NASA Space Radiation Program Element Discipline Lead Scientist for the Cardiovascular/Degenerative Tissue Risk.

Lisa Simonsen, PhD, is a scientist at NASA Langley Research Center, Hampton, VA, and is the Human Research Program Element Scientist for the NASA Space Radiation Program Element.

Honglu Wu, PhD, is a scientist at NASA Johnson Space Center, Houston, TX.

IX. LIST OF ACRONYMS

ARRBOD	Acute Radiation Risk and BRYNTRN Organ Dose
ARS	Acute Radiation Syndrome
BFO	Blood Forming Organ
CAF	Computerized Anatomical Female
CAM	Computerized Anatomical Male
CME	Coronal Mass Ejection
CNS	Central Nervous System
DNA	DeoxyriboNucleic acid
DoD	Department of Defense
ED10	Dose at which 10% of the population receive the effect
EVA	ExtraVehicular Activity
F	Solar modulation parameter
FAX	Female Adult voXel mode
FW	Fatigue/Weakness
GCR	Galactic Cosmic Rays
GI	GastroIntestinal
GOES	Geostationary Operational Environmental Satellite
Gy	Gray
Gy-Eq	Gray-equivalent
HSC	Hematopoietic Stem Cell
HU	Hindlimb Unloaded
HZE	High Charge and Energy
ICRP	International Commission on Radiological Protection
IL	Interleukin
IRP	Integrated Research Plan
IVA	IntraVehicular Activity
LD50	median Lethal Dose
LET	Linear Energy Transfer
MAX	Male Adult voXel model
MeV	Megaelectron Volt
mGy	milliGray

mSv	milliSievert
NAS	National Academy of Sciences
NCRP	National Council on Radiation Protection and Measurements
NOAA	National Oceanographic and Atmospheric Agency's
NRC	Nuclear Regulatory Commission
NUREG	NUclear REGulations from NRC
PEL	Permissible Exposure Limit
RBE	Relative Biological Effectiveness
SPE	Solar Particle Event
TGF	Transforming Growth Factor
TNF	Tumor Necrosis Factor
UGID	Upper Gastro Intestinal Distress